

Beyond Hard Constraints: Budget-Conditioned Reachability For Safe Offline Reinforcement Learning

Janaka Chathuranga Brahmanage and Akshat Kumar

School of Computing and Information Systems, Singapore Management University.
janakat.2022@phdcs.smu.edu.sg, akshatkumar@smu.edu.sg

Abstract

Sequential decision-making using Markov Decision Process underpins many real-world applications. Both model-based and model-free methods have achieved strong results in these settings. However, real-world tasks must balance reward maximization with safety constraints, often conflicting objectives, that can lead to unstable min–max, adversarial optimization. A promising alternative is *safety reachability* analysis, which precomputes a forward-invariant safe state–action set, ensuring that an agent starting inside this set remains safe indefinitely. Yet, most reachability-based methods address only hard safety constraints, and little work extends reachability to cumulative cost constraints. To address this, *first*, we define a safety-conditioned reachability set that *decouples* reward maximization from cumulative safety cost constraints. *Second*, we show how this set enforces safety constraints without unstable min–max or Lagrangian optimization, yielding a novel offline safe RL algorithm that learns a safe policy from a fixed dataset without environment interaction. *Finally*, experiments on standard offline safe-RL benchmarks, and a real-world maritime navigation task demonstrate that our method matches or outperforms state-of-the-art baselines while maintaining safety.

Code — <https://github.com/janakact/bcrl>

1 Introduction

Markov Decision Processes (MDPs) have demonstrated impressive success modeling across a range of domains, including robotics (Tang et al. 2024), algorithm discovery (Fawzi et al. 2022), classical board games (Silver et al. 2016), and Atari games (Mnih et al. 2013). Despite these achievements, deploying agents in real-world settings poses significant challenges. In practice, most of the applications utilize a Reinforcement Learning (RL) framework to train agents, and these agents must not only maximize cumulative reward but also operate safely (Altman 2021), requiring policies that strike a balance between performance and safety. Additionally, constructing fast and accurate simulators for complex environments is often computationally prohibitive. Offline safe reinforcement learning (*offline safe RL*) offers a practical solution by enabling agents to learn from

pre-collected datasets without further environment interaction (Liu et al. 2024). This work aims to develop methods that address the dual goals of reward optimization and safety in offline RL, an important problem in RL research (Gu et al. 2024).

Related work Constrained Markov decision processes (CMDPs) (Altman 2021) are a standard framework for safe RL. Prior offline safe RL methods often struggle with optimization instability or high computational overhead. Lagrangian methods like BCQ-Lagrangian (Liu et al. 2024) and min-max approaches like CPQ (Xu, Zhan, and Zhu 2022) suffer from tuning difficulties and unstable learning. Methods like COptiDICE (Lee et al. 2022) perform distribution correction but struggle empirically on recent benchmarks (Liu et al. 2024). Recent approaches learn generative models (VAEs) as a pre-training step (Koirala et al. 2025; Guo et al. 2025), which incurs significant computational overhead. Alternatively, Hamilton-Jacobi (HJ) reachability (Ganai, Gao, and Herbert 2024; Zheng et al. 2024; Yu et al. 2022) enforces safety independently of the policy but has mainly focused on hard constraints rather than cumulative costs. Another related approach, Saute RL (Sootla et al. 2022), enforces per-step constraints but requires online rollouts to track budgets. In contrast, our approach prunes unsafe actions offline using a dynamic budget without requiring a generative model or online samples. We provide an extended discussion of related work in Appendix C.

Adaptive Safty Budgets for RL Standard safe RL methods enforce static, episode-level constraints (i.e., *expected* cost over all the episodes is less than a budget). In contrast, we introduce a step-wise budget that dynamically adjusts during policy execution. A key benefit is that using this step-wise budget, we can prune unsafe actions at each time step and guide value estimation (for both reward and cost), enabling policy that adapts over time.

Our contributions are:

- We propose **Budget-Conditioned Reachability**, a framework that applies reachability analysis to CMDPs with cumulative cost constraints. It uses dynamic budgets to estimate persistently safe state–action sets, enabling reward-maximizing policy learning within this safe region. We also provide rigorous theoretical justification for the framework.



Figure 1: Electronic navigation chart for maritime traffic navigation in Singapore strait

- We introduce two variants of our method to address both deterministic and stochastic CMDP settings, ensuring broad applicability across different problem structures.
- Our method integrates seamlessly with existing offline RL algorithms such as IQL (Wang et al. 2023), XQL (Garg et al. 2023), and SparseQL (Xu et al. 2023), yielding a safe offline RL approach, **BCRL** (Budget-Conditioned Reachability RL). The resulting algorithms are easy to implement, require no min-max adversarial training, never query out-of-distribution actions, and generalize to any budget.
- We evaluate BCRL on interpretable grid-world environments, DSRL benchmarks (Liu et al. 2024), and a real-world maritime navigation task, where agents are trained using historical ship trajectory data to navigate safely in high-traffic conditions. Extensive ablations show consistent improvements over state-of-the-art baselines.

2 Preliminaries

2.1 Constrained Markov Decision Process

A constrained Markov Decision Process (CMDP) is defined as a tuple $\mathcal{M} := \langle S, A, T, r, c, \gamma, \mu_0, \delta_{\text{init}} \rangle$. Here, S and A represent the state and action spaces, respectively. The transition dynamics are given by $T(s' | s, a)$, specifying the probability of transitioning from state s to s' under action a . The reward function is $r(s, a) : S \times A \rightarrow \mathbb{R}$, and the cost function is $c(s, a) : S \times A \rightarrow \mathbb{R}^+$. The discount factor is $\gamma \in [0, 1)$, and the initial state distribution is $\mu_0 : S \rightarrow [0, 1]$. The δ_{init} is the cost threshold over the total expected cost agent can incur under any policy. **The objective** is to determine a policy $\pi : S \rightarrow \Delta(A)$ that maximizes the expected discounted reward $J_R(\pi)$, subject to the cost constraint $J_C(\pi) \leq \delta_{\text{init}}$ where,

$$J_R(\pi) = \mathbb{E}_{\pi} \sum_{t=0}^{\infty} \gamma^t r(s_t, a_t); \quad J_C(\pi) = \mathbb{E}_{\pi} \sum_{t=0}^{\infty} \gamma^t c(s_t, a_t) \quad (1)$$

and $\delta_{\text{init}} \in [0, \delta_{\text{max}}]$ is the cost (or safety budget) threshold. Here $\delta_{\text{max}} = \frac{c_{\text{max}}}{1-\gamma}$, where c_{max} is the highest cost the environment can incur at a single step.

Learning from offline data For CMDPs, getting faithful domain model (e.g., transition, reward, cost functions) for realistic problems is challenging. Thus, we focus on the offline RL setting where we learn from a pre-collected transition dataset $\mathcal{D} = \{(s_i, a_i, r(s_i, a_i), c(s_i, a_i), s'_i)\}_{i=1}^N$ generated by one or more behavioral policies π_{β} . Offline safe RL

aims to learn a policy π that optimizes CMDP objective subject to cost constraints using this dataset alone, without further environment interaction. As a real world example, consider the safe maritime navigation problem in figure 1. The Singapore strait is a high traffic, constrained waterway, with vessels navigating narrow lanes, TSS corridors, anchorage zones, and areas near landmasses. Ships must make sequential decisions—adjusting speed or heading—while avoiding restricted zones, minimizing collision risk, and following navigation rules. Because unsafe exploration is impossible in real waters, learning through trial-and-error is not feasible. Yet, the sea traffic generates extensive AIS (automatic identification system) data on vessel positions, speeds, headings, and interactions. This makes safe offline RL a natural fit for such problems where safe policies are learned solely from historical data without real-world experimentation.

2.2 In-Sample Q-learning Algorithms

For *unconstrained* RL, several algorithms use asymmetric loss functions to estimate the value function instead of the exact maximum, learning policies from offline data without querying unseen Q-values. They employ expectile regression to fit the Bellman optimal value, replacing the max operator while still following temporal-difference learning. The critic $Q_{\theta}(s, a)$, target critic $Q_{\theta_T}(s, a)$, and value function $V_{\psi}(s)$, parameterized by θ , θ_T , and ψ , are trained by minimizing the following losses:

$$\mathcal{L}^V(\psi) = \mathbb{E}_{(s,a) \sim \mathcal{D}} [\mathcal{L}^*(Q_{\theta_T}(s, a) - V_{\psi}(s))] \quad (2)$$

$$\mathcal{L}^Q(\theta) = \mathbb{E}_{(s,a,s') \sim \mathcal{D}} [(r(s, a) + \gamma V_{\psi}(s') - Q_{\theta}(s, a))^2] \quad (3)$$

Here, L^* is an asymmetric loss approximating the maximum Q-value. In IQL (Kostrikov, Nair, and Levine 2022), $L^*(u) = L^{\tau}(u) = |\tau - \mathbf{1}_{\{u < 0\}}|u^2$ is the expectile loss (Newey and Powell 1987), with $\tau > 0.5$ penalizing positive errors more, pushing $V_{\psi}(s)$ toward the maximum. XQL (Garg et al. 2023) uses Gumbel regression, and SparseQL (Xu et al. 2023) introduces a robust asymmetric loss. Target parameters are updated via $\theta_T \leftarrow (1 - \alpha)\theta_T + \alpha\theta$. These methods are computationally efficient, avoid querying OOD actions, and have strong theoretical guarantees (Kostrikov, Nair, and Levine 2022; Xu et al. 2023). For policy extraction, they use in-sample methods similar to Advantage Weighted Regression (AWR) (Peng et al. 2019). In this work, we adopt primarily in-sample methods to avoid OOD actions.

2.3 Persistent Safety with Value Functions

In safe RL, we sometimes have access to a safety indicator for a given state, which can be viewed as a state-wise safety constraint. However, it is not sufficient to ensure only *instantaneous safety*. When an agent takes an action, we also need to guarantee that in the future the agent will always have at least one safe action available. In other words, the agent should not be driven into an unrecoverable situation or a dead end. A safety signal that indicates the agent is not in an unrecoverable state is referred to as a *persistent safety*

signal (Yu et al. 2022). Hamilton–Jacobi (HJ) reachability-based RL methods (Zheng et al. 2024; Yu et al. 2022; Ganai et al. 2023) address this by estimating a *forward-invariant safety set*. This set consists of states from which the agent can remain safe indefinitely, provided it follows an appropriate policy. For example, in FISOR (Zheng et al. 2024), the immediate safety indicator $h(s)$ defines the safe state set $S_f := \{s \in S \mid h(s) \leq 0\}$. A learned value function is then used to estimate

$$V_h^*(s) = \min_{\pi} V_h^{\pi}(s) = \min_{\pi} \max_{t \in \mathbb{N}} h(s_t) \quad (4)$$

If $V_h^*(s) \leq 0$, this implies that there exists a policy π such that the future cost satisfies $V_h^{\pi}(s) \leq 0$. Therefore, V_h^* acts as a persistent safety indicator. The set $S_p := \{s \in S \mid V_h^*(s) \leq 0\}$ is then used to define the persistent safety set.

3 Budget-Conditioned Reachability

Prior reachability and persistent safety estimation methods are mostly limited to hard constraints (i.e., whether safety indicator $h(s) \leq 0$). They do not extend trivially to cumulative cost based safety constraints in CMDPs. Thus, we aim to estimate the persistent safety set *independently* of the policy being learned, using it to enforce cumulative cost constraints. Decoupling safety estimation from policy optimization ensures the learned policy remains safe while making learning more stable and tractable, without using Lagrangian or min-max adversarial optimization. Our approach builds on three key ideas: **(1)** augmenting the CMDP to explicitly track the remaining budget, **(2)** estimating a budget-conditioned persistent safety set for *any* remaining budget, and **(3)** solving the augmented CMDP.

3.1 A Budget-Conditioned Persistent Safety Set

Similar to the definition of persistent safety discussed in Section 2.3, we now define the budget-conditioned safety set that indicate feasibility based on the discounted future cost.

Definition 3.1 (The optimal cost-value function). *The optimal state-cost-value function V_C^* and the optimal action-cost-value function Q_C^* are defined as:*

$$V_C^*(s) = \min_{\pi} V_C^{\pi}(s) = \min_{\pi} \mathbb{E}_{\substack{\pi \\ s_0=s}} \sum_{t \in \mathbb{N}} \gamma^t c(s_t, a_t), \quad (5)$$

$$Q_C^*(s, a) = \min_{\pi} Q_C^{\pi}(s, a) = \min_{\substack{\pi \\ s_0=s \\ a_0=a}} \mathbb{E}_{\pi} \sum_{t \in \mathbb{N}} \gamma^t c(s_t, a_t) \quad (6)$$

Following a similar reasoning as in Section 2.3, we claim that, given a budget δ , if $V_C^*(s) \leq \delta$, then there exists a policy π such that the future discounted cost satisfies $V_C^{\pi}(s) \leq \delta$. Therefore, $V_C^*(s) \leq \delta$ serves as a persistent safety indicator for the given budget, guaranteeing that there exists a policy under which the future cost remains within the budget. This allows us to define the largest set of feasible states, as well as the feasible actions for each state, that remain within the given budget.

Definition 3.2 (Budget-Conditioned Persistent Safety Sets). *Given a budget δ , the budget-conditioned persistent safety set is defined as:*

$$S_P(\delta) := \{s \in S \mid V_C^*(s) \leq \delta\}. \quad (7)$$

Similarly, the budget-conditioned persistent safe action set for a given state s is defined as:

$$A_P(s, \delta) := \{a \in A \mid Q_C^*(s, a) \leq \delta\}. \quad (8)$$

Intuitively, the budget-conditioned persistent safety set consists of states where a policy exists to keep the total discounted future cost within the budget δ .

Lemma 3.3 (Safe Actions Always Exist for Persistent Safety States). *Given $\delta \in \mathbb{R}^+$; for any state $s \in S_P(\delta)$, the budget-conditioned persistent safe action set $A_P(s, \delta)$ is non-empty: $A_P(s, \delta) \neq \emptyset$.*

Proof. Let $s \in S_P(\delta)$, which means by definition $V_C^*(s) \leq \delta$. By the definition of the value function,

$$V_C^*(s) = \min_{\pi} \mathbb{E} \left[\sum_{t=0}^{\infty} \gamma^t c(s_t, a_t) \mid s_0 = s, \pi \right] = \min_{a \in A} Q_C^*(s, a),$$

so there exists at least one action $a^* \in A$ that attains this minimum. Therefore, $Q_C^*(s, a^*) = V_C^*(s) \leq \delta$, which implies $a^* \in A_P(s, \delta)$. Hence, $A_P(s, \delta) \neq \emptyset$. \square

In the following sections, we discuss how the budget-conditioned persistent safety sets defined above can be used to enforce the cumulative cost constraint of the CMDP.

3.2 Budget Adaptive MDPs

Since the definition of the budget-conditioned persistent safety set depends on the remaining budget, it is necessary to make the budget an explicit part of the system’s dynamics. To achieve this, we extend the CMDP by augmenting its state space with a dynamic budget variable. This augmentation allows the agent to reason about safety not only as a function of the environment state but also as a function of the available safety budget over time. One key contribution is our method for initializing and updating the budget via functions f and g . Specially for stochastic MDPs, these updates are non-trivial and crucial for ensuring the theoretical guarantees of our approach.

Definition 3.4 (Budget-Adaptive MDP). *A Budget-Adaptive Markov Decision Process (BAMDP) constructed from a CMDP \mathcal{M} is a tuple*

$$\bar{\mathcal{M}}(\mathcal{M}, f, g) := \langle \bar{S}, A, \bar{T}, \bar{r}, \bar{c}, \gamma, \bar{\mu}_0, \delta_{init} \rangle.$$

where the augmented state space is $\bar{S} := S \times \mathbb{R}^+$, and the action space A remain unchanged. The reward and cost functions are unchanged from the original CMDP. That is, $\bar{r}((s, \delta), a) := r(s, a)$, $\bar{c}((s, \delta), a) := c(s, a)$.

The initial budget function $f : S \times \mathbb{R}^+ \rightarrow \mathbb{R}^+$ assigns the initial budget based on the CMDP budget δ_{init} and the starting state s_0 , such that the augmented initial state distribution is:

$$\bar{\mu}_0 := \{(s_0, \delta_0) \mid s_0 \sim \mu_0, \delta_0 = f(s_0, \delta_{init})\}.$$

The budget update function $g : S \times A \times S \times \mathbb{R}^+ \rightarrow \mathbb{R}^+$ updates the budget after each transition. In the most general form considered here, it depends on the current state s , action a , next state s' , and the current budget δ , such that

$\delta' = g(s, a, s', \delta)$. This results in the following augmented transition function:

$$\bar{T}((s', \delta') | (s, \delta), a) := T(s' | s, a) \cdot \mathbf{1}_{\{\delta' = g(s, a, s', \delta)\}},$$

where $\mathbf{1}_{\{\cdot\}}$ is the indicator function.

Intuition of f and g The role of f and g is to initialize and track a remaining budget (or a similar quantity) while executing the policy, and then use it to prune the action space, as discussed later in this section. The simplest setup is to define $f(s_0, \delta_{\text{init}}) := \delta_{\text{init}}$, $g(s, a, s', \delta) := \frac{\delta - c(s, a)}{\gamma}$, where the budget is initialized as the CMDP cost constraint. This formulation keeps track of the exact remaining budget while dividing by γ to account for discounting. However, this is not the only possible formulation. We can also track other quantities as the budget, as long as they help enforce the original CMDP cost constraint. In Section 3.4, we show how such a quantity can be utilized in stochastic CMDPs.

While we present our formulation with a single cost objective, our approach naturally extends to multiple cost types by augmenting the state space with a budget vector. We provide the detailed formulation for multiple cost constraints in Appendix A.3.

Definition 3.5 (Budget-Restricted Policy Set). Let $A_P(s, \delta)$ denote the persistent safety action set, as defined in the Eq (8). The budget-restricted policy set is:

$$\Pi_P := \left\{ \pi : \bar{S} \rightarrow \Delta(A) \mid \pi(a | (s, \delta)) > 0 \implies a \in A_P(s, \delta) \right\}$$

The goal of defining Π_P is that, with an appropriate choice of f and g , any policy in Π_P will satisfy the CMDP constraint, as discussed in Section 3.3 and Section 3.4.

The objective of the BAMDP is to find a policy in Π_P that maximizes the reward.

$$\pi^* = \max_{\pi \in \Pi_P} \mathbb{E} \sum_{t=0}^{\infty} \gamma^t \bar{r}((s_t, \delta_t), a_t) \quad (9)$$

Feasible state space and Π_P A policy in Π_P may not be defined for all states, since there may exist states where $Q_C^*(s, a) > \delta$ for all actions $a \in A$, leaving no admissible action. The following definition identifies the subset of states where the budget-restricted policy set Π_P can be well-defined.

Definition 3.6 (Feasible State Subspace). The feasible state subspace is $\bar{S}_P := \left\{ (s, \delta) \mid \delta \in \mathbb{R}^+, s \in S_P(\delta) \right\}$. where $S_P(\delta)$ is the persistent safety set in (7).

Augmented State Space: Figure 2 illustrates the modified state space and the feasible subspace defined within it. The feasible subspace represents the set of augmented states $((s, \delta))$ where each state (s) remains feasible under its corresponding budget (δ) . As shown in Lemma 3.3, for every state $s \in S_P(\delta)$, the safe action set $A_P(s, \delta)$ is non-empty. This guarantees that the policy set Π_P is well-defined over \bar{S}_P , since there is always at least one admissible action for each $(s, \delta) \in \bar{S}_P$.

Intuitively, some key desirable properties associated with \bar{S}_P and Π_P are: (a) the set \bar{S}_P should be persistent. That,

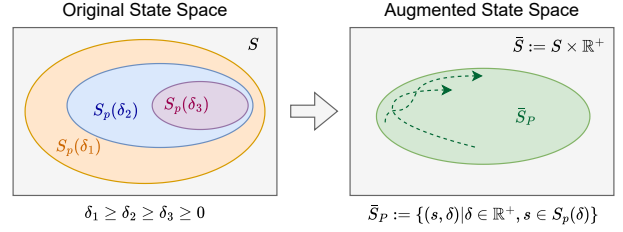


Figure 2: State augmentation with budget. A desirable property is set \bar{S}_P to be persistent (trajectories starting in \bar{S}_P must end in \bar{S}_P)

is an agent starting in $s \in \bar{S}_P$ remains in \bar{S}_P following a policy $\pi \in \Pi_P$; (b) For any policy $\pi \in \Pi_P$, it is guaranteed that the original CMDP constraint $J_C(\pi) \leq \delta_{\text{init}}$ is satisfied. We show in sections 3.3 and 3.4 how to choose appropriate budget update functions for these properties to hold.

Benefits of defining Π_P and \bar{S}_P : Both sets are constructed from the persistent safety sets in Eq. 7 and Eq. 8, which depend only on the conservative cost critic and are independent of both the reward signal and the reward-optimizing policy. This makes enforcing $\pi \in \Pi_P$ far simpler than satisfying the original CMDP constraint in Eq. 1, which depends on the policy being learned and creates a difficult min–max coupling between the cost critic, reward critic, and policy. Our formulation removes this circular dependency, yielding a more stable learning process.

3.3 Budget Update for Deterministic CMDPs

We begin with the deterministic setting, which provides clearer intuition. To define budget-conditioned safety set, we need to specify how the safety budget evolves along a state-action trajectory. In deterministic CMDPs, where transitions and trajectories are uniquely determined by the policy and environment dynamics, this evolution can be defined directly through a budget update rules below.

Definition 3.7 (Direct Budget-Tracking). Let $\bar{\mathcal{M}}_D$ denote the Direct Budget Tracking BAMDP defined by

$$\bar{\mathcal{M}}_D(\mathcal{M}) := \bar{\mathcal{M}}(\mathcal{M}, f, g).$$

Budget update functions are:

$$f(s_0, \delta_{\text{init}}) = \delta_{\text{init}}, \quad g(s, a, s', \delta) = \frac{\delta - c(s, a)}{\gamma}.$$

This formulation keeps track of the remaining budget, and the division by γ accounts for the discounting effect of the CMDP constraint. In a deterministic environment, we next show that tracking such a budget and using it to select safe actions based on the persistent safety set A_P can enforce the original cumulative cost constraint of the CMDP, as shown in the following theorem.

Theorem 3.8. Let $\bar{\mathcal{M}}_D(\mathcal{M})$ be the Direct Budget-Tracking BAMDP defined above, and assume the underlying CMDP \mathcal{M} is deterministic with cost budget $\delta_{\text{init}} \geq V_C^*(s_0)$. Then,

1. Any policy $\pi \in \Pi_P$ induces trajectories that start in and remain entirely within the feasible subspace \bar{S}_P .
2. Any deterministic policy π satisfying the CMDP cost constraint (Eq. 1) belongs to Π_P .

3. Conversely, if $\pi \in \Pi_P$, then it satisfies the cumulative cost constraint of the underlying CMDP \mathcal{M} .

Therefore, in deterministic environments, it is sufficient to enforce $\pi \in \Pi_P$ instead of explicitly enforcing the cumulative cost constraint.

The proof of the above theorem is provided in the appendix A.1. This result highlights a key property of this construction: in deterministic settings, enforcing persistent safety via the direct budget-tracking BAMDP is equivalent to satisfying the original cumulative cost constraint. This result formally links the concept of persistent safety to standard CMDP feasibility, showing that any policy constrained to remain within the safe set automatically respects the cumulative cost limit. Therefore, as discussed in the previous section, during training we can restrict the policy to select actions only from the persistent safe action set A_P (8), without explicitly enforcing the cumulative cost constraint (1).

3.4 Budget Update for Stochastic CMDPs

The conditions described in the previous section no longer hold in a stochastic MDP. In particular, in a stochastic setting, the cost-to-go satisfies

$$Q_C^*(s, a) = c(s, a) + \gamma \mathbb{E}_{s'}[V_C^*(s')],$$

rather than the deterministic form $Q_C^*(s, a) = c(s, a) + \gamma V_C^*(s')$. As a result, the next-state value $V_C^*(s')$ can take a range of values, and the budget update defined for the deterministic setting no longer guarantees that (s', δ') lies inside \tilde{S}_P . In such cases, we may need to follow a different policy—possibly the most conservative policy at these states—but doing so does not ensure that the agent will satisfy the CMDP constraint in Eq. (1).

To address these issues, we propose an alternative budget update formulation, called *soft budget-tracking*.

Definition 3.9 (Soft Budget-Tracking). Let $\bar{\mathcal{M}}_S$ denote the Soft Budget-Tracking BAMDP defined by

$$\bar{\mathcal{M}}_S(\mathcal{M}) := \bar{\mathcal{M}}(\mathcal{M}, f, g),$$

with

$$f(s_0, \delta_{init}) = V_C^*(s_0) + \delta_{init} - \mathbb{E}_{s \sim \mu_0}[V_C^*(s)], \quad (10)$$

$$g(s, a, s', \delta) = V_C^*(s') + \frac{\delta - Q_C^*(s, a)}{\gamma} \quad (11)$$

The advantage of the above formulation is that it ensures that after any transition, the next state $(s', \delta') \in \tilde{S}_P$. Moreover, we can show that it satisfies the CMDP constraint.

Although $\bar{\mathcal{M}}_S$ may seem unintuitive, it reduces to the budget update in $\bar{\mathcal{M}}_D$ under fully deterministic settings, as shown in the following lemma.

Lemma 3.10 (Reduction to Deterministic Budget-Tracking). In a fully deterministic setting, the soft budget-tracking BAMDP $\bar{\mathcal{M}}_S$ simplifies to the direct budget-tracking BAMDP $\bar{\mathcal{M}}_D$.

The proof of Lemma 3.10 is provided in Appendix A.2. With the soft budget-tracking BAMDP, we can reason about

the behavior of policies constrained to remain within the persistent safety set \tilde{S}_P , even in stochastic environments. Under the reasonable assumption Eq. (12) on the initial cost threshold, we can formally show that these policies maintain feasibility: they remain inside the persistent safety set and satisfy the CMDP cumulative cost constraint in expectation. The following theorem summarizes these key properties.

Theorem 3.11 (Properties of Policies in Π_P under Soft Budget-Tracking). Let $\bar{\mathcal{M}}_S$ be the soft budget-tracking BAMDP. Assume the CMDP is feasible, i.e., the cost threshold δ_{init} satisfies

$$\delta_{init} \geq \mathbb{E}_{s \sim \mu_0}[V_C^*(s)]. \quad (12)$$

Let $\pi \in \Pi_P$, and define the expected discounted cumulative cost from an augmented state $(s, \delta) \in \tilde{S}$ by

$$J_C^\pi((s, \delta)) := \mathbb{E}_\pi \left[\sum_{t=0}^{\infty} \gamma^t c(s_t, a_t) \mid (s_0, \delta_0) = (s, \delta) \right].$$

Then the following properties hold:

1. Any policy $\pi \in \Pi_P$ induces trajectories that start in and remain entirely within the feasible subspace \tilde{S}_P .
2. For any $(s, \delta) \in \tilde{S}_P$ and any policy $\pi \in \Pi_P$, $J_C^\pi((s, \delta)) \leq \delta$.
3. Any policy $\pi \in \Pi_P$ satisfies the CMDP cumulative cost constraint (Eq. 1): $J_C(\pi) \leq \delta_{init}$.

The proof of Theorem 3.11 is provided in Appendix A.2. The theorem ensures that any policy in Π_P remains within \tilde{S}_P and that the expected cumulative cost from any augmented state (s, δ) does not exceed its budget δ , thereby satisfying the CMDP constraint. Unlike the deterministic case, we cannot guarantee that all CMDP-feasible policies lie within Π_P , so the resulting constraint may be stricter. Nevertheless, our empirical results show that it still yields high-quality policies.

CMDP Instantiation We next discuss how to formulate and solve BAMDP from a given CMDP with known model. BAMDP is formed by augmenting the state with a discretized budget dimension and defining transitions using f or g , depending on whether the setting is stochastic or deterministic. We mask states outside \tilde{S}_P and restrict actions to the support of Π_P . The resulting finite MDP can then be solved with a standard LP solver. Further details appear in Appendix D.1.

In real-world settings where dynamics are unknown, offline RL is often used to learn from pre-collected data. Next, we show how our framework integrates with standard offline RL methods to solve *constrained* RL problems.

4 Safe Offline-RL With BAMDP

In this section we discuss how our approach can be used with existing *unconstrained* offline RL algorithms. Our approach can be seen as a two step process:

1. Learn persistent safety sets S_P and A_P by estimating V_C^* and Q_C^* that minimize cumulative cost, ignoring the reward, in the original MDP \mathcal{M} .

- Train an Offline RL agent to maximize the reward for the augmented MDP $\bar{\mathcal{M}}$, while ensuring that the resulting policy respects the persistent safety constraints.

The first step is performed on the original MDP, while the second step is defined on the BAMDP.

Learning the Persistent Safety Set For the first step, any offline RL algorithm can be used; the only difference is that we minimize the cost instead of maximizing the reward. In practice, in-sample RL algorithms such as IQL (Kostrikov, Nair, and Levine 2022), XQL (Garg et al. 2023), or SparseQL (Xu et al. 2023) are particularly convenient, as they do not require learning a policy to estimate Q-values. However, if one wishes to use algorithms that rely on out-of-distribution actions, such as SAC+BC (Fujimoto and Gu 2021), CQL (Kumar et al. 2020), our approach is fully compatible and does not impose any restrictions. For convenience and stability, we use IQL in our implementation. The following loss functions can then be used, with $\tau_C \leq 0.5$ to minimize the cost (details in (Kostrikov, Nair, and Levine 2022)):

$$\mathcal{L}_C^V(\psi) = \mathbb{E}_{(s,a) \sim \mathcal{D}} [\mathcal{L}^{\tau_C}(Q_{\theta_T}^C(s,a) - V_{\psi}^C(s))] \quad (13)$$

$$\mathcal{L}_C^Q(\theta) = \mathbb{E}_{(s,a,s') \sim \mathcal{D}} [(c(s,a) + \gamma V_{\psi}^C(s') - Q_{\theta}^C(s,a))^2] \quad (14)$$

Offline RL within the Augmented MDP In this step, we train an RL algorithm within the persistent safety set of the augmented MDP $\bar{\mathcal{M}}(\mathcal{M}, f, g)$, ensuring the policy selects only actions from A_P by restricting the MDP to \bar{S}_P . To facilitate training, we define an augmented dataset as follows:

$$\bar{\mathcal{D}} := \left\{ \left(\underbrace{(s, \delta)}_{\bar{s}}, a, \underbrace{(s', \delta')}_{\bar{s}'} \right) \mid \delta \sim \mathcal{U}_{[Q_C^*(s,a), \delta_{\max}]}, \delta' = g(s,a,s',\delta) \right\}$$

Unlike a fixed dataset, this augmented dataset is not pre-generated; instead, we sample mini-batches from it dynamically during training. Here, the budget δ is sampled from a uniform distribution $\mathcal{U}_{[Q_C^*(s,a), \delta_{\max}]}$ to generate augmented transitions within the persistent safety set. Sampling $\delta \geq Q_C^*(s,a)$ ensures that the dataset extends only to the persistent safety set \bar{S}_P and not to the full augmented state space \bar{S} . The rewards $r(s,a)$ and $c(s,a)$ remain unchanged, as discussed in the Definition 3.4.

Implicit Enforcement of Persistent Safety Offline RL naturally stays close to the behavior policy, thus restricting the dataset to the persistent safety set already biases the learned policy to remain within it. In practice, we found no extra penalties are required.

IQL-Instantiation We instantiate our approach using Implicit Q-Learning (IQL) by extending the offline dataset to include only transitions within the persistent safety set \bar{S}_P . This modification naturally integrates our safety constraint into the learning process. The value and Q-functions are trained using the standard expectile regression (with $\tau_R \geq 0.5$) and Bellman objectives defined over the augmented dataset $\bar{\mathcal{D}}$:

$$\mathcal{L}_R^V(\hat{\psi}) = \mathbb{E}_{(\bar{s}, a, \bar{s}') \sim \bar{\mathcal{D}}} [\mathcal{L}^{\tau_R}(Q_{\hat{\theta}_T}^R(\bar{s}, a) - V_{\hat{\psi}}^R(\bar{s}))] \quad (15)$$

Algorithm 1: BCRL : IQL Instantiation Algorithm

Initialize Parameters: $\theta, \theta_T, \psi, \hat{\theta}, \hat{\theta}_T, \hat{\psi}, \phi$
Inputs: Offline data \mathcal{D} , and other hyper parameters $\tau_c, \tau_r, \alpha, \beta$
for each gradient step do
 $(s, a, s') \sim \mathcal{D}$ \triangleright sample mini batch of transitions
 $\theta \leftarrow \theta - \lambda_Q^C \nabla_{\theta} \mathcal{L}_C^Q(\theta)$ \triangleright update cost-critic Eq.(14)
 $\psi \leftarrow \psi - \lambda_V^C \nabla_{\psi} \mathcal{L}_C^V(\psi)$ \triangleright update cost-value Eq.(13)
 $\theta_T \leftarrow (1 - \alpha)\theta_T + \alpha\theta$ \triangleright soft update cost target-net.

 $\delta \sim \mathcal{U}_{[Q_{\theta}^C(s,a), \delta_{\max}]}$ \triangleright sample budget from uniform dist.
 $\delta' = g(s, a, s', \delta)$ \triangleright compute next budget
 $\bar{s} = (s, \delta)$ and $\bar{s}' = (s', \delta')$ \triangleright compute augmented states
 $\hat{\theta} \leftarrow \hat{\theta} - \lambda_Q^R \nabla_{\hat{\theta}} \mathcal{L}_R^Q(\hat{\theta})$ \triangleright update reward critic Eq.(16)
 $\hat{\psi} \leftarrow \hat{\psi} - \lambda_V^R \nabla_{\hat{\psi}} \mathcal{L}_R^V(\hat{\psi})$ \triangleright update value function Eq.(15)
 $\hat{\theta}_T \leftarrow (1 - \alpha)\hat{\theta}_T + \alpha\hat{\theta}$ \triangleright soft update reward target-net.
 $\phi \leftarrow \phi - \lambda_{\pi} \nabla_{\phi} \mathcal{L}^{\pi R}(\phi)$ \triangleright policy extraction (AWR) Eq.(17)
end for

$$\mathcal{L}_R^Q(\hat{\theta}) = \mathbb{E}_{(\bar{s}, a, \bar{s}') \sim \bar{\mathcal{D}}} [(\bar{r}(\bar{s}, a) + \gamma V_{\hat{\psi}}^R(\bar{s}') - Q_{\hat{\theta}}^R(\bar{s}, a))^2] \quad (16)$$

Here, θ_T denotes the target network parameters, which are updated using a soft update. For policy extraction, we follow Advantage-Weighted Regression (AWR) as in IQL, where the policy is trained to maximize the advantage-weighted likelihood of actions under the Q-function:

$$\mathcal{L}^{\pi}(\phi) = - \mathbb{E}_{(\bar{s}, a) \sim \bar{\mathcal{D}}} \left[\exp \left(\frac{A(\bar{s}, a)}{\beta} \right) \log \pi_{\phi}(a | \bar{s}) \right] \quad (17)$$

where $A(\bar{s}, a) = Q_{\hat{\theta}}^R(\bar{s}, a) - V_{\hat{\psi}}^R(\bar{s})$ denotes the advantage, and β controls the temperature of the weighting distribution. The exact learning process is outlined in the Algorithm 1. In our method, called BCRL, cost critics (Q^C, V^C) can be learned by ignoring rewards altogether, and policy extraction only depends on reward critics. This is significantly more stable than standard Lagrangian relaxation methods.

5 Experiments

We evaluate BCRL on DSRL benchmarks (Liu et al. 2024) and a real-world maritime navigation task. We aim to answer following questions: **(Q1)** Does BCRL create a notable gap from the optimal CMDP (model known) solution, particularly under stochastic conditions? (Section 5.1) **(Q2)** Can BCRL outperform existing state-of-the-art offline (model-free) safe RL baselines on standard benchmarks? (Section 5.2) **(Q3)** How sensitive is BCRL to different hyperparameter settings, and how do these choices affect its performance and safety behavior? **(Q4)** How does BCRL behave on real-world-data, both qualitatively (in terms of safe and interpretable trajectories) and quantitatively (in terms of performance and safety metrics)? (Section 5.3).

Baselines and benchmarks: For our main results, we compare against state-of-the-art baselines that also generalize to different cost budgets similar to our method. These methods include **CDT** (Liu et al. 2023), **CAPS** (Chemingui et al. 2025), **CCAC** (Guo et al. 2025), and **LSPC** (Koirala et al.

	CDT		CAPS		CCAC		LSPC		BCRL (Ours)	
	reward \uparrow	cost \downarrow	reward \uparrow	cost \downarrow	reward \uparrow	cost \downarrow	reward \uparrow	cost \downarrow	reward \uparrow	cost \downarrow
PointButton1	0.53 \pm 0.01	1.68 \pm 0.13	0.04 \pm 0.15	0.58 \pm 1.42	0.68 \pm 0.14	4.31 \pm 3.20	0.09 \pm 0.20	0.69 \pm 1.03	0.07 \pm 0.18	0.79 \pm 2.10
PointButton2	0.46 \pm 0.01	1.57 \pm 0.10	0.12 \pm 0.20	0.96 \pm 2.35	0.63 \pm 0.11	4.82 \pm 3.61	0.19 \pm 0.21	1.39 \pm 2.53	0.12 \pm 0.22	0.81 \pm 1.36
PointCircle1	0.59 \pm 0.00	0.69 \pm 0.04	0.50 \pm 0.12	0.68 \pm 1.51	0.58 \pm 0.13	2.22 \pm 1.05	0.56 \pm 0.35	3.49 \pm 3.55	0.55 \pm 0.17	0.86 \pm 0.21
PointCircle2	0.64 \pm 0.01	1.05 \pm 0.08	0.51 \pm 0.21	0.76 \pm 0.47	0.18 \pm 0.50	1.42 \pm 1.09	0.67 \pm 0.24	4.18 \pm 4.56	0.58 \pm 0.10	0.74 \pm 0.34
PointGoal1	0.69 \pm 0.02	1.12 \pm 0.07	0.46 \pm 0.28	0.63 \pm 0.81	0.55 \pm 0.26	1.88 \pm 1.72	0.26 \pm 0.27	0.23 \pm 0.45	0.56 \pm 0.25	0.70 \pm 0.65
PointGoal2	0.59 \pm 0.03	1.34 \pm 0.05	0.34 \pm 0.23	0.80 \pm 0.74	0.41 \pm 0.36	3.60 \pm 3.37	0.23 \pm 0.24	0.50 \pm 0.79	0.38 \pm 0.21	0.77 \pm 0.68
CarCircle1	0.60 \pm 0.01	1.73 \pm 0.04	0.55 \pm 0.16	1.54 \pm 1.63	0.49 \pm 0.14	5.13 \pm 3.53	0.46 \pm 0.25	1.86 \pm 3.14	0.50 \pm 0.12	0.48 \pm 0.43
SwimmerVelocity	0.66 \pm 0.01	0.96 \pm 0.08	0.44 \pm 0.22	1.66 \pm 2.37	-0.08 \pm 0.02	0.00 \pm 0.01	0.46 \pm 0.21	1.28 \pm 2.60	0.49 \pm 0.18	0.99 \pm 0.37
HopperVelocity	0.63 \pm 0.06	0.61 \pm 0.08	0.44 \pm 0.26	0.75 \pm 0.83	0.46 \pm 0.38	0.50 \pm 0.55	0.21 \pm 0.04	1.25 \pm 1.20	0.66 \pm 0.23	0.80 \pm 0.35
SafetyGym Average (21 tasks)	0.54 \pm 0.21	1.06 \pm 0.59	0.36 \pm 0.34	0.76 \pm 1.43	0.41 \pm 0.46	3.18 \pm 5.24	0.34 \pm 0.19	1.10 \pm 1.75	0.38 \pm 0.17	0.57 \pm 0.68
BallRun	0.39 \pm 0.09	1.16 \pm 0.19	0.18 \pm 0.09	0.94 \pm 0.73	0.40 \pm 0.12	0.84 \pm 0.31	0.15 \pm 0.01	0.00 \pm 0.00	0.20 \pm 0.02	0.06 \pm 0.10
AntRun	0.72 \pm 0.04	0.91 \pm 0.42	0.61 \pm 0.13	0.78 \pm 0.59	0.12 \pm 0.09	0.04 \pm 0.08	0.66 \pm 0.13	1.43 \pm 1.25	0.68 \pm 0.11	0.95 \pm 0.29
BallCircle	0.77 \pm 0.06	1.07 \pm 0.27	0.69 \pm 0.10	0.59 \pm 0.23	0.78 \pm 0.05	0.46 \pm 0.31	0.62 \pm 0.28	1.17 \pm 1.95	0.69 \pm 0.11	0.97 \pm 0.27
CarCircle	0.75 \pm 0.06	0.95 \pm 0.61	0.70 \pm 0.10	0.66 \pm 0.27	0.72 \pm 0.04	0.77 \pm 0.44	0.78 \pm 0.12	1.88 \pm 3.23	0.53 \pm 0.17	0.51 \pm 0.51
DroneCircle	0.63 \pm 0.07	0.98 \pm 0.27	0.55 \pm 0.06	0.65 \pm 0.29	0.29 \pm 0.27	0.63 \pm 0.70	0.60 \pm 0.02	1.31 \pm 0.86	0.42 \pm 0.12	0.52 \pm 0.32
AntCircle	0.54 \pm 0.20	1.78 \pm 4.33	0.37 \pm 0.18	0.15 \pm 0.25	0.61 \pm 0.14	0.75 \pm 0.90	0.44 \pm 0.14	0.53 \pm 0.93	0.56 \pm 0.17	0.79 \pm 0.60
BulletGym Average (8 tasks)	0.68 \pm 0.19	1.04 \pm 1.65	0.57 \pm 0.25	0.86 \pm 1.82	0.54 \pm 0.30	1.07 \pm 2.04	0.60 \pm 0.10	1.01 \pm 1.35	0.58 \pm 0.09	0.67 \pm 0.46
easysparse	0.17 \pm 0.14	0.23 \pm 0.32	0.12 \pm 0.20	0.37 \pm 0.43	-0.06 \pm 0.00	0.10 \pm 0.05	0.79 \pm 0.14	1.34 \pm 1.43	0.70 \pm 0.19	0.94 \pm 0.17
easymeans	0.45 \pm 0.11	0.54 \pm 0.55	0.02 \pm 0.07	0.21 \pm 0.23	-0.06 \pm 0.01	0.07 \pm 0.08	0.82 \pm 0.06	1.33 \pm 0.86	0.73 \pm 0.17	0.94 \pm 0.13
easymean	0.32 \pm 0.18	0.62 \pm 0.43	0.11 \pm 0.15	0.16 \pm 0.17	-0.06 \pm 0.00	0.07 \pm 0.04	0.84 \pm 0.10	1.88 \pm 1.20	0.70 \pm 0.17	0.90 \pm 0.16
mediumsparse	0.87 \pm 0.11	1.10 \pm 0.26	0.59 \pm 0.36	0.74 \pm 0.97	-0.08 \pm 0.00	0.07 \pm 0.04	0.97 \pm 0.02	1.24 \pm 0.68	0.94 \pm 0.07	0.82 \pm 0.32
mediummean	0.45 \pm 0.39	0.75 \pm 0.83	0.66 \pm 0.35	0.90 \pm 0.89	-0.07 \pm 0.01	0.02 \pm 0.03	0.93 \pm 0.12	0.78 \pm 0.51	0.92 \pm 0.11	0.77 \pm 0.16
mediumdense	0.88 \pm 0.12	2.41 \pm 0.71	0.75 \pm 0.29	0.65 \pm 0.57	-0.08 \pm 0.00	0.06 \pm 0.03	0.82 \pm 0.30	1.07 \pm 0.71	0.78 \pm 0.28	0.68 \pm 0.31
hardmean	0.33 \pm 0.21	0.97 \pm 0.31	0.29 \pm 0.13	0.28 \pm 0.31	-0.05 \pm 0.00	0.06 \pm 0.03	0.48 \pm 0.14	1.16 \pm 1.19	0.46 \pm 0.15	0.84 \pm 0.54
harddense	0.08 \pm 0.15	0.21 \pm 0.42	0.36 \pm 0.18	0.66 \pm 0.92	-0.03 \pm 0.01	0.11 \pm 0.08	0.47 \pm 0.19	1.43 \pm 0.93	0.44 \pm 0.17	0.63 \pm 0.24
MetaDrive Average (9 tasks)	0.42 \pm 0.31	0.80 \pm 0.61	0.38 \pm 0.34	0.54 \pm 0.69	-0.06 \pm 0.02	0.07 \pm 0.06	0.74 \pm 0.13	1.24 \pm 0.89	0.69 \pm 0.16	0.81 \pm 0.27

Table 1: **Results for normalized cost and normalized reward:** \uparrow indicates that a higher value is better, while \downarrow indicates that a lower value is preferable. **Bold** text denotes safe policies, gray indicates unsafe policies, and **blue** highlights the highest reward among the safe policies for each task. Each result is obtained by running three random seeds across three distinct cost thresholds and evaluating over 20 episodes. Some tasks are omitted to save space. Complete results are provided in Table 3 of Appendix B.

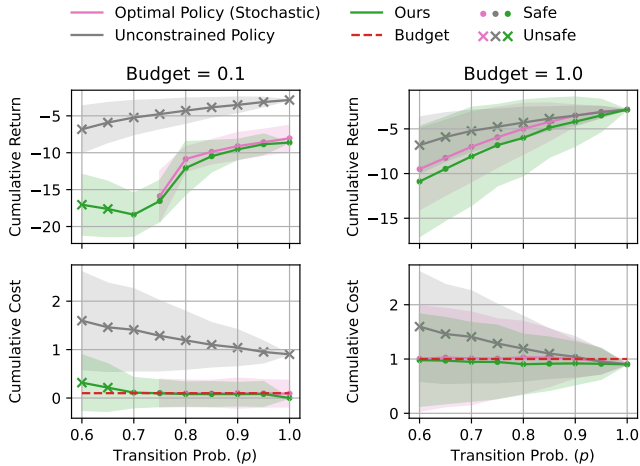


Figure 3: **Comparison with Optimal Solution:** Grid-world results with X-axis as the intended-movement probability p (higher values indicate less noise). Top plots show total return; bottom plots show cost for two budget levels.

2025). An additional comparison with methods that do not adapt to different cost budgets is provided in the supplementary. We use the DSRL (Liu et al. 2024) dataset and environments. We evaluate our approach on all 38 tasks, which include three types of environments: *SafetyGym*, *BulletGym*, and *MetaDrive*. The evaluation metrics include *Normalized-Reward* and *Normalized-Cost*, where the cost is normalized with respect to the cost threshold; that is, *Normalized-*

Cost > 1 indicates an unsafe policy. More details on these metrics are in the Appendix.

5.1 Synthetic CMDPs

Under deterministic dynamics, our method matches the optimal solution; in stochastic settings, it can be slightly conservative. We test this on a discrete grid world where the optimal CMDP policy is computed via Linear Programming (LP) solvers. The agent starts at a fixed point and must reach a goal (appendix C.7 provides environment details.). Figure 3 compares our method with the LP solution and an unconstrained baseline. The X-axis is the probability of executing the intended action; lower values introduce more randomness. When this probability is too low, no feasible policy satisfies the budget, so the LP solver yields no solution (shown as missing plot segments). For all the cases, both methods satisfy the cost constraint, and our approach incurs only a small reward gap. As the environment becomes less noisy, our solution converges to the LP optimum. This shows that even in a highly stochastic setting, BCRL is fairly accurate.

5.2 Offline Safe RL

Main Results. Table 1 reports the main results under the standard DSRL evaluation settings. All algorithms are trained following the official DSRL benchmark protocols, with additional implementation details provided in the Appendix. We instantiate BCRL using IQL. In stochastic domains (e.g., *SafetyGym*, *Bullet-SafetyGym*), we use the stochastic variant, while for deterministic environments like

	ADE (m) ↓	Close quarters Rate ↓	Avg. Acceleration (ms^{-2})	Avg. Speed (ms^{-1})	Success Rate ↑
EXPERT	0.0	0.3	0.0001	4.44	1.0
CAPS	87.3 ± 19.82	0.23 ± 0.05	0.0034 ± 0.0006	5.67 ± 0.07	0.73 ± 0.16
CCAC	371.07 ± 26.74	0.11 ± 0.06	0.7549 ± 0.1339	21.41 ± 0.0	0.0 ± 0.0
LSPC	251.61 ± 22.68	0.17 ± 0.02	0.0087 ± 0.0157	8.47 ± 0.37	0.23 ± 0.1
BCRL	52.08 ± 10.64	0.26 ± 0.03	-0.0006 ± 0.0003	3.65 ± 0.14	0.88 ± 0.03

Table 2: Performance metrics in the Maritime Navigation Task (section 5.3)

MetaDrive, we report the deterministic version. Both variant results are detailed in the Appendix for completeness. Overall, the results show BCRL consistently outperforms baselines while satisfying safety across all domains. BCRL produces safe policies in all 38 out of 38 tasks (indicated in **bold**), outperforming all baselines in 16 out of 38 tasks, and achieving strongly consistent results as highlighted in **blue**. BCRL attains **highest average performance across all three benchmarks**.

Table 1 focuses on baselines capable of adapting to different cost budgets. Additional comparisons with non-budget-conditioned baselines such as BC-Safe (Liu et al. 2024), BCQ-Lag, COptiDICE (Lee et al. 2022), and CPQ (Xu, Zhan, and Zhu 2022) are in the Appendix B. **Runtime:** Our algorithm was tested on an NVIDIA RTX 3090 GPU. As shown in Table 9 (in appendix), it completes training and evaluation within a few minutes—significantly faster than baseline methods that require 2–3 hours under the same conditions. Although runtime comparisons are approximate, the results indicate notable efficiency gains of our method.

Ablations: Our IQL variant is governed by three hyperparameters: the cost critic expectile (τ_C), the reward critic expectile (τ_R), and the AWR policy temperature (β). Among these, the expectile values influence performance more, as also noted in (Kostrikov, Nair, and Levine 2022). Expectile ablation results are in Table 6, appendix C.4. Additionally, the appendix discusses how the quality of the learned cost critic affects overall performance and how inclusive the learned persistent safety set is.

5.3 Evaluation on Real-World Maritime Data

We test BCRL on a real-world maritime navigation task, learning a policy that imitates expert captains navigating congested routes while minimizing collision risk. We use the maritime traffic simulator, and the imitation-learning dataset from (Pham, Brahmanage, and Kumar 2025), augmented with reward and cost signals. The agent receives a sparse reward of 100 for reaching the goal, and a cost of 1 for entering a **close-quarter scenario** (getting close to another vessel within 555m (Pham, Brahmanage, and Kumar 2025)).

The dataset contains ~ 2 years of AIS trajectories from vessels operating in the Singapore Strait. We simulate a **multi-agent environment** where surrounding vessels replay their historical (log-play) paths, while the RL-controlled ego agent starts from a historical position but must follow its learned policy. The agent observes the past five steps of its own and nearby vessels’ states and uses a delta-action space (Gulino et al. 2023). We evaluate performance using

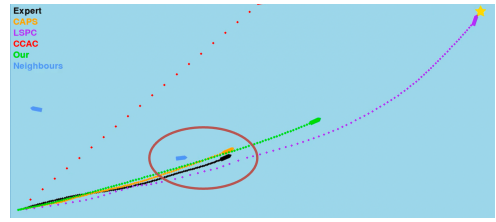


Figure 4: Expert, learned trajectories in marine navigation

the **average displacement error (ADE)**, the **close-quarter rate**, and the **success rate**. To model dense traffic, we select the top 20% most congested scenarios. We additionally report **average acceleration and speed** to assess how closely the policy matches real-world maneuvering. Further environment and dataset details appear in Appendix C.3.

As shown in Table 2, BCRL reduces close-quarter events from 30% to 26%—a meaningful improvement given the high-risk nature of close encounters involving large cargo and tanker vessels. BCRL also achieves the **lowest ADE** (~ 52 m) and the highest **success rate** (88%). Some baselines reduce close-quarter rates further but at the cost of unrealistic deviations from expert trajectories or reduced task success. In contrast, BCRL maintains expert-like **acceleration and speed** profiles. Results are averaged over 3 seeds with 100 evaluation episodes each.

Figure 4 illustrates qualitative behavior: the expert’s trajectory (dotted **black**), neighboring vessels (**blue**), and learned-policy rollouts—**BCRL**, **LSPC**, **CCAC**, and **CAPS**. The red ellipse shows a close-quarter scenario where the expert gets too close to a **neighbor**. BCRL avoids near-misses through smooth path and speed adjustments, whereas LSPC and CCAC exhibit unrealistic deviations. CAPS performs more reasonably but shows higher acceleration and lower success than BCRL. Additional results and videos are included in the supplementary material.

6 Conclusion

We introduced **Budget-Conditioned Reachability (BCR)**, a novel framework that fundamentally decouples reward maximization from cumulative safety constraints in Constrained Markov Decision Processes (CMDPs). By defining a dynamic, safety-conditioned reachability set—tracked through a step-wise remaining budget—our approach prunes unsafe actions at each timestep and ensures reliable constraint satisfaction without resorting to unstable min-max adversarial optimization or computationally heavy generative models.

A significant advantage of our framework is its plug-and-play compatibility with any standard offline RL algorithm (e.g., IQL), enabling the cost critics to be learned independently of the reward for improved training stability. Through extensive cross-domain validation—ranging from interpretable grid-worlds and the high-dimensional DSRL benchmark to a complex, real-world maritime navigation task—BCRL consistently matches or exceeds state-of-the-art performance while reliably ensuring safety.

References

- Altman, E. 2021. *Constrained Markov Decision Processes: Stochastic Modeling*. Boca Raton: Routledge, 1 edition. ISBN 978-1-315-14022-3.
- Chemingui, Y.; Deshwal, A.; Wei, H.; Fern, A.; and Doppa, J. R. 2025. Constraint-Adaptive Policy Switching for Offline Safe Reinforcement Learning. In *AAAI*, volume 39, 15722–15730.
- Chen, L.; Lu, K.; Rajeswaran, A.; Lee, K.; Grover, A.; Laskin, M.; Abbeel, P.; Srinivas, A.; and Mordatch, I. 2021. Decision Transformer: Reinforcement Learning via Sequence Modeling. In *NeurIPS*, volume 34, 15084–15097.
- Fawzi, A.; Balog, M.; Huang, A.; Hubert, T.; Romera-Paredes, B.; Barekatin, M.; Novikov, A.; R. Ruiz, F. J.; Schrittwieser, J.; Swirszcz, G.; Silver, D.; Hassabis, D.; and Kohli, P. 2022. Discovering faster matrix multiplication algorithms with reinforcement learning. *Nature*, 610(7930): 47–53.
- Fujimoto, S.; and Gu, S. S. 2021. A Minimalist Approach to Offline Reinforcement Learning. arXiv:2106.06860.
- Ganai, M.; Gao, S.; and Herbert, S. L. 2024. Hamilton-Jacobi Reachability in Reinforcement Learning: A Survey. *IEEE Open Journal of Control Systems*, 3: 310–324.
- Ganai, M.; Gong, Z.; Yu, C.; Herbert, S.; and Gao, S. 2023. Iterative Reachability Estimation for Safe Reinforcement Learning. ArXiv:2309.13528 [cs].
- Garg, D.; Hejna, J.; Geist, M.; and Ermon, S. 2023. Extreme Q-Learning: MaxEnt RL without Entropy. In *ICLR*.
- Gu, S.; Yang, L.; Du, Y.; Chen, G.; Walter, F.; Wang, J.; and Knoll, A. 2024. A Review of Safe Reinforcement Learning: Methods, Theory and Applications. In *IEEE Transactions on Pattern Analysis and Machine Intelligence*.
- Gulino, C.; Fu, J.; Luo, W.; Tucker, G.; Bronstein, E.; Lu, Y.; Harb, J.; Pan, X.; Wang, Y.; Chen, X.; Co-Reyes, J. D.; Agarwal, R.; Roelofs, R.; Lu, Y.; Montali, N.; Mougín, P.; Yang, Z.; White, B.; Faust, A.; McAllister, R.; Anguelov, D.; and Sapp, B. 2023. Waymax: An Accelerated, Data-Driven Simulator for Large-Scale Autonomous Driving Research. In *Proceedings of Thirty-seventh Conference on Neural Information Processing Systems*.
- Guo, Z.; Zhou, W.; Wang, S.; and Li, W. 2025. Constraint-Conditioned Actor-Critic for Offline Safe Reinforcement Learning. In *ICLR*.
- Kingma, D. P.; Welling, M.; et al. 2019. An introduction to variational autoencoders. *Foundations and Trends® in Machine Learning*, 12(4): 307–392.
- Koirala, P.; Jiang, Z.; Sarkar, S.; and Fleming, C. 2025. Latent Safety-Constrained Policy Approach for Safe Offline Reinforcement Learning. In *ICLR*.
- Kostrikov, I.; Nair, A.; and Levine, S. 2022. Offline Reinforcement Learning with Implicit Q-Learning. In *ICLR*.
- Kumar, A.; Zhou, A.; Tucker, G.; and Levine, S. 2020. Conservative Q-Learning for Offline Reinforcement Learning. ArXiv:2006.04779 [cs, stat].
- Lee, J.; Paduraru, C.; Mankowitz, D. J.; Heess, N.; Precup, D.; Kim, K.-E.; and Guez, A. 2022. COptiDICE: Offline Constrained Reinforcement Learning via Stationary Distribution Correction Estimation. In *ICLR*.
- Liu, Z.; Guo, Z.; Lin, H.; Yao, Y.; Zhu, J.; Cen, Z.; Hu, H.; Yu, W.; Zhang, T.; Tan, J.; and Zhao, D. 2024. Datasets and Benchmarks for Offline Safe Reinforcement Learning. *JMLR*.
- Liu, Z.; Guo, Z.; Yao, Y.; Cen, Z.; Yu, W.; Zhang, T.; and Zhao, D. 2023. Constrained Decision Transformer for Offline Safe Reinforcement Learning. In *ICML*.
- Mnih, V.; Kavukcuoglu, K.; Silver, D.; Graves, A.; Antonoglou, I.; Wierstra, D.; and Riedmiller, M. 2013. Playing Atari with Deep Reinforcement Learning.
- Newey, W. K.; and Powell, J. L. 1987. Asymmetric Least Squares Estimation and Testing. *Econometrica*, 55(4): 819–847.
- Peng, X. B.; Kumar, A.; Zhang, G.; and Levine, S. 2019. Advantage-Weighted Regression: Simple and Scalable Off-Policy Reinforcement Learning.
- Pham, Q. A.; Brahmanage, J. C.; and Kumar, A. 2025. Ship-NaviSim: Data-Driven Simulation for Real-World Maritime Navigation. In *AAMAS*, 1641–1649. Richland, SC: International Foundation for Autonomous Agents and Multiagent Systems. ISBN 979-8-4007-1426-9.
- Silver, D.; Huang, A.; Maddison, C. J.; Guez, A.; Sifre, L.; van den Driessche, G.; Schrittwieser, J.; Antonoglou, I.; Panneershelvam, V.; Lanctot, M.; Dieleman, S.; Grewe, D.; Nham, J.; Kalchbrenner, N.; Sutskever, I.; Lillicrap, T.; Leach, M.; Kavukcuoglu, K.; Graepel, T.; and Hassabis, D. 2016. Mastering the game of Go with deep neural networks and tree search. *Nature*, 529(7587): 484–489.
- Sootla, A.; Cowen-Rivers, A. I.; Jafferjee, T.; Wang, Z.; Mguni, D.; Wang, J.; and Bou-Ammar, H. 2022. Saute RL: Almost Surely Safe Reinforcement Learning Using State Augmentation. In *ICML*.
- Tang, C.; Abbatematteo, B.; Hu, J.; Chandra, R.; Martín-Martín, R.; and Stone, P. 2024. Deep Reinforcement Learning for Robotics: A Survey of Real-World Successes. In *Annual Review of Control, Robotics, and Autonomous Systems*.
- Wang, X.; Xu, H.; Zheng, Y.; and Zhan, X. 2023. Offline Multi-Agent Reinforcement Learning with Implicit Global-to-Local Value Regularization. In *NeurIPS*.
- Xu, H.; Jiang, L.; Li, J.; Yang, Z.; Wang, Z.; Chan, V. W. K.; and Zhan, X. 2023. Offline RL with No OOD Actions: In-Sample Learning via Implicit Value Regularization. In *ICLR*.
- Xu, H.; Zhan, X.; and Zhu, X. 2022. Constraints Penalized Q-learning for Safe Offline Reinforcement Learning. In *NeurIPS*.
- Yu, D.; Ma, H.; Li, S. E.; and Chen, J. 2022. Reachability Constrained Reinforcement Learning. In *ICML*.
- Zheng, Y.; Li, J.; Yu, D.; Yang, Y.; Li, S. E.; Zhan, X.; and Liu, J. 2024. Safe Offline Reinforcement Learning with Feasibility-Guided Diffusion Model. In *ICLR*.

A Theoretical Results

A.1 Deterministic Case

Theorem 3.8. Let $\bar{\mathcal{M}}_D(\mathcal{M})$ be the Direct Budget-Tracking BAMDP defined above, and assume the underlying CMDP \mathcal{M} is deterministic with cost budget $\delta_{\text{init}} \geq V_C^*(s_0)$. Then,

1. Any policy $\pi \in \Pi_P$ induces trajectories that start in and remain entirely within the feasible subspace \bar{S}_P .
2. Any deterministic policy π satisfying the CMDP cost constraint (Eq. 1) belongs to Π_P .
3. Conversely, if $\pi \in \Pi_P$, then it satisfies the cumulative cost constraint of the underlying CMDP \mathcal{M} .

Therefore, in deterministic environments, it is sufficient to enforce $\pi \in \Pi_P$ instead of explicitly enforcing the cumulative cost constraint.

Proof. Let $\bar{\mathcal{M}}_{\text{Det}}(\mathcal{M})$ and notation be as above, and assume \mathcal{M} is deterministic. Denote by $(s_t, a_t)_{t \geq 0}$ the state-action sequence induced by a deterministic policy π started at s_0 , and let $c_t := c(s_t, a_t)$. Recall the direct budget update $\delta_{t+1} = \frac{\delta_t - c_t}{\gamma}$, $\delta_0 = \delta_{\text{init}}$.

(1) Any $\pi \in \Pi_P$ induces trajectories that remain in \bar{S}_P . Let $\pi \in \Pi_P$ and consider the trajectory starting from (s_0, δ_0) . By assumption, $V_C^*(s_0) \leq \delta_{\text{init}}$, and since $\delta_0 = \delta_{\text{init}}$, it follows that $s_0 \in S_P(\delta_0)$. Since $\pi \in \Pi_P$ we get $Q_C^*(s_0, a_0) \leq \delta_0$. Using the bellman-identity $Q_C^*(s_0, a_0) = c_0 + \gamma V_C^*(s_1)$ we obtain

$$V_C^*(s_1) = \frac{Q_C^*(s_0, a_0) - c_0}{\gamma} \leq \frac{\delta_0 - c_0}{\gamma} = \delta_1.$$

Since cost is always positive, $V_C^*(s_1) \geq 0$, which implies $\delta_1 \in \mathbb{R}^+$ and $s_1 \in S_P(\delta_1)$. Therefore, by definition, $(s_1, \delta_1) \in \bar{S}_P$. Moreover, there exists at least one action at s_1 with $Q_C^*(\cdot) \leq \delta_1$. Repeating the same argument at each step shows that all subsequent augmented states (s_t, δ_t) remain in \bar{S}_P . Thus, trajectories under π never leave \bar{S}_P .

(2) If π satisfies the cumulative cost constraint then $\pi \in \Pi_P$. Assume the policy π satisfies the cumulative cost constraint in \mathcal{M} , i.e.

$$J(\tau) = \sum_{t=0}^{\infty} \gamma^t c_t \leq \delta_{\text{init}} = \delta_0.$$

Unrolling the budget recursion gives the identity

$$\gamma^t \delta_t = \delta_0 - \sum_{i=0}^{t-1} \gamma^i c_i \quad (t \geq 1),$$

hence, since $J(\tau) \leq \delta_0$,

$$\gamma^t \delta_t \geq \sum_{k=t}^{\infty} \gamma^k c_k = \gamma^t \sum_{k=t}^{\infty} \gamma^{k-t} c_k.$$

Dividing by γ^t yields

$$\delta_t \geq \sum_{k=t}^{\infty} \gamma^{k-t} c_k \quad (=: R_t),$$

where R_t is the actual remaining discounted cost from time t . For the deterministic MDP we have for the chosen action

$$Q_C^*(s_t, a_t) = c(s_t, a_t) + \gamma V_C^*(s_{t+1}),$$

and since $V_C^*(s_{t+1})$ is the *minimal* possible remaining cost from s_{t+1} , it holds that $V_C^*(s_{t+1}) \leq \sum_{k=t+1}^{\infty} \gamma^{k-(t+1)} c(s_k, a_k)$. Therefore

$$Q_C^*(s_t, a_t) \leq c(s_t, a_t) + \gamma \sum_{k=t+1}^{\infty} \gamma^{k-(t+1)} c_k = R_t \leq \delta_t.$$

Thus at every visited augmented state (s_t, δ_t) the chosen action satisfies $Q_C^*(s_t, a_t) \leq \delta_t$, so $\pi \in \Pi_P$.

(3) If $\pi \in \Pi_P$ then π satisfies the cumulative cost constraint. Assume $\pi \in \Pi_P$, i.e. for every t the chosen action satisfies $Q_C^*(s_t, a_t) \leq \delta_t$. By the direct budget update we have equality

$$c(s_t, a_t) = \delta_t - \gamma \delta_{t+1},$$

so multiplying by γ^t and summing over $t \geq 0$ gives the telescoping series

$$\sum_{t=0}^T \gamma^t c(s_t, a_t) = \sum_{t=0}^T (\gamma^t \delta_t - \gamma^{t+1} \delta_{t+1}) = \delta_0 - \gamma^{T+1} \delta_{T+1}.$$

Since $\delta_{T+1} \geq 0$ for all T , letting $T \rightarrow \infty$ yields

$$\sum_{t=0}^{\infty} \gamma^t c(s_t, a_t) \leq \delta_0,$$

so the cumulative cost constraint holds.

Conclusion. Combining (1)–(3) we obtain the claimed equivalence in the deterministic setting: enforcing $\pi \in \Pi_P$ is both necessary and sufficient for satisfying the cumulative cost constraint, and any policy in Π_P produces trajectories that stay in \bar{S}_P . Therefore, in deterministic environments it suffices to enforce $\pi \in \Pi_P$ instead of directly enforcing the cumulative cost constraint. \square

A.2 Stochastic Case

Lemma 3.10 (Reduction to Deterministic Budget-Tracking). *In a fully deterministic setting, the soft budget-tracking BAMDP $\bar{\mathcal{M}}_S$ simplifies to the direct budget-tracking BAMDP $\bar{\mathcal{M}}_D$.*

Proof. In a deterministic MDP, a well trained cost critic satisfies $Q_C^*(s, a) = c(s, a) + \gamma V_C^*(s')$ since there is no stochasticity and the Bellman equation reduces to the deterministic form. Substituting this into the soft budget-tracking update:

$$g(s, a, s', \delta) = V_C^*(s') + \frac{\delta - Q_C^*(s, a)}{\gamma} = \frac{\delta - c(s, a)}{\gamma},$$

which is exactly the budget update defined in the direct budget-tracking CMDP $\bar{\mathcal{M}}_D$.

Similarly in the deterministic setting $V_C^*(s_0) = \mathbb{E}_{s \sim \mu_0} [V_C^*(s)]$. Therefore, the initial budget:

$$f(s_0, \delta_{\text{init}}) = V_C^*(s_0) + \delta_{\text{init}} - \mathbb{E}_{s \sim \mu_0} [V_C^*(s)] = \delta_{\text{init}},$$

Thus, $\bar{\mathcal{M}}_S$ reduces to $\bar{\mathcal{M}}_D$ in the deterministic setting. \square

Theorem 3.11. *Let $\bar{\mathcal{M}}_S$ be the soft budget-tracking BAMDP. Assume the CMDP is feasible, i.e., the cost threshold δ_{init} satisfies*

$$\delta_{\text{init}} \geq \mathbb{E}_{s \sim \mu_0} [V_C^*(s)].$$

Let $\pi \in \Pi_P$, and define the expected discounted cumulative cost from an augmented state $(s, \delta) \in \bar{S}$ by

$$J_C^\pi((s, \delta)) := \mathbb{E}_\pi \left[\sum_{t=0}^{\infty} \gamma^t c(s_t, a_t) \mid (s_0, \delta_0) = (s, \delta) \right].$$

Then the following properties hold:

1. Any policy $\pi \in \Pi_P$ induces trajectories that start in and remain entirely within the feasible subspace \bar{S}_P .
2. For any $(s, \delta) \in \bar{S}_P$ and any policy $\pi \in \Pi_P$, $J_C^\pi((s, \delta)) \leq \delta$.
3. Any policy $\pi \in \Pi_P$ satisfies the CMDP cumulative cost constraint (Eq. 1): $J_C(\pi) \leq \delta_{\text{init}}$.

Proof. We prove each property separately:

1. Trajectories remain in \bar{S}_P . Consider any policy $\pi \in \Pi_P$ and the augmented state trajectory $\{(s_t, \delta_t)\}_{t \geq 0}$ it induces. From Assumption 12, we have $\delta_{\text{init}} \geq \mathbb{E}_{s \sim \mu_0} [V_C^*(s)]$. Substituting this into the budget initialization function f gives,

$$\delta_0 = V_C^*(s_0) + \delta_{\text{init}} - \mathbb{E}_{s \sim \mu_0} [V_C^*(s)] \geq V_C^*(s_0),$$

and therefore $s_0 \in S_P$, and $(s_0, \delta_0) \in \bar{S}_P$.

At each time step t , the policy selects an action $a_t \in A_P(\delta_t)$, which ensures $Q_C^*(s_t, a_t) \leq \delta_t$. The budget update in $\bar{\mathcal{M}}_S$ gives

$$\delta_{t+1} = V_C^*(s_{t+1}) + \frac{\delta_t - Q_C^*(s_t, a_t)}{\gamma} \geq V_C^*(s_{t+1}),$$

so $(s_{t+1}, \delta_{t+1}) \in \bar{S}_P$.

By induction, all subsequent augmented states remain in \bar{S}_P . Therefore, trajectories under any $\pi \in \Pi_P$ start in and remain entirely within the feasible subspace \bar{S}_P .

2. Pointwise budget satisfaction. Fix an augmented state $(s, \delta) \in \bar{S}_P$ and a policy $\pi \in \Pi_P$. By $(s, \delta) \in \bar{S}_P$ we have $s \in S_P(\delta)$ and $\delta \geq V_C^*(s)$, and by $\pi \in \Pi_P$ the support condition $\text{supp } \pi(\cdot | (s, \delta)) \subseteq \{a : Q_C^*(s, a) \leq \delta\}$ holds.

Define the finite-horizon truncated action-value in the augmented CMDP:

$$Q_C^{\pi, h}((s, \delta), a) := \mathbb{E}_\pi \left[\sum_{t=0}^h \gamma^t c(s_t, a_t) \mid (s_0, \delta_0) = (s, \delta), a_0 = a \right],$$

and the truncated state-value

$$V_C^{\pi, h}((s, \delta)) := \mathbb{E}_{a \sim \pi(\cdot | (s, \delta))} [Q_C^{\pi, h}((s, \delta), a)].$$

We show by induction on the horizon h that for every action a and every $h \geq 0$,

$$Q_C^{\pi, h}((s, \delta), a) \leq \delta. \quad (18)$$

Base ($h = 0$). $Q_C^{\pi, 0}((s, \delta), a) = c(s, a)$. Since $c(s, a) \leq Q_C^*(s, a)$ and actions in the support satisfy $Q_C^*(s, a) \leq \delta$, we get $Q_C^{\pi, 0}((s, \delta), a) \leq \delta$.

Inductive step. Assume (18) holds for horizon h . Consider horizon $h + 1$. Using the recursion for truncated values and the soft budget update $\delta' = V_C^*(s') + \frac{\delta - Q_C^*(s, a)}{\gamma}$, we have

$$\begin{aligned} Q_C^{\pi, h+1}((s, \delta), a) &= c(s, a) + \gamma \mathbb{E}_{s' \sim T(\cdot | s, a)} [V_C^{\pi, h}((s', \delta'))] \\ &\leq c(s, a) + \gamma \mathbb{E}_{s'} [\delta'] \quad (\text{by the inductive hypothesis applied at each } (s', \delta')) \\ &= c(s, a) + \gamma \mathbb{E}_{s'} \left[V_C^*(s') + \frac{\delta - Q_C^*(s, a)}{\gamma} \right] \\ &= c(s, a) + \gamma \mathbb{E}_{s'} [V_C^*(s')] + (\delta - Q_C^*(s, a)) \\ &= Q_C^*(s, a) + (\delta - Q_C^*(s, a)) \quad (\text{Bellman equation for } Q_C^*) \\ &= \delta, \end{aligned}$$

so (18) holds for $h + 1$.

Pass to the limit. Letting $h \rightarrow \infty$ (justified by $\gamma \in [0, 1)$ and nonnegative bounded costs) yields

$$Q_C^\pi((s, \delta), a) \leq \delta \quad \forall a \in A,$$

and therefore

$$V_C^\pi((s, \delta)) = \mathbb{E}_{a \sim \pi(\cdot | (s, \delta))} [Q_C^\pi((s, \delta), a)] \leq \delta. \quad (19)$$

By definition $J_C^\pi((s, \delta)) = V_C^\pi((s, \delta))$, hence $J_C^\pi((s, \delta)) \leq \delta$. This holds for every $(s, \delta) \in \bar{S}_P$, proving the theorem.

3. Global CMDP feasibility Based on the budget initialization function for every s_0 the initialized budget

$$\delta_0 = V_C^*(s_0) + \delta_{\text{init}} - \mathbb{E}_{s \sim \mu_0} [V_C^*(s)]$$

Taking expectation over $s_0 \sim \mu_0$ gives

$$J_C(\pi) = \mathbb{E}_{(s_0, \delta_0) \sim \bar{\mu}_0} [J_C^\pi((s_0, \delta_0))] \quad (20)$$

$$= \mathbb{E}_{(s_0, \delta_0) \sim \bar{\mu}_0} [V_C^\pi((s_0, \delta_0))] \quad (21)$$

$$\leq \mathbb{E}_{(s_0, \delta_0) \sim \bar{\mu}_0} [\delta_0] \quad \text{From Eq. 19} \quad (22)$$

$$= \mathbb{E}_{s_0 \sim \mu_0} [V_C^*(s_0) + \delta_{\text{init}} - \mathbb{E}_{s \sim \mu_0} [V_C^*(s)]] \quad (23)$$

$$= \delta_{\text{init}}. \quad (24)$$

This completes the proof and shows that $\pi \in \Pi_P$ satisfy the cumulative cost constraint in the underlying CMDP. \square

A.3 Extension to Multiple Cost Objectives

In many real-world applications, agents must satisfy multiple distinct safety constraints simultaneously (e.g., avoiding collisions while maintaining battery levels). Our *Budget-Conditioned Reachability* (BCRL) framework naturally extends to this setting by augmenting the state space with a *budget vector*. Let there be N distinct cost functions $\{c_i\}_{i=1}^N$, where each $c_i : S \times A \rightarrow \mathbb{R}^+$, and a corresponding vector of initial cost thresholds $\delta_{init} = [\delta_{init,1}, \dots, \delta_{init,N}]^T$.

Augmented State Space The augmented state space is defined as $\bar{S} := S \times (\mathbb{R}^+)^N$. A state is represented as (s, δ) , where $\delta \in \mathbb{R}^N$ tracks the remaining budget for each constraint independently.

Persistent Safety Set Intersection The budget-conditioned persistent safety set is defined as the intersection of the feasible sets for each individual cost objective. For a budget vector δ , the safe state set is:

$$S_P(\delta) := \bigcap_{i=1}^N \{s \in S \mid V_{C_i}^*(s) \leq \delta_i\} \quad (25)$$

Similarly, the safe action set $A_P(s, \delta)$ is the intersection of actions safe for all objectives:

$$A_P(s, \delta) := \bigcap_{i=1}^N \{a \in A \mid Q_{C_i}^*(s, a) \leq \delta_i\} \quad (26)$$

Vectorized Budget Initialization and Update The budget is initialized and updated using vector-valued functions \mathbf{f} and \mathbf{g} , which generalize the scalar functions from the main text.

The initialization is given by $\delta_0 = \mathbf{f}(s_0, \delta_{init})$, where $\mathbf{f} : S \times (\mathbb{R}^+)^N \rightarrow (\mathbb{R}^+)^N$. Typically, this operates element-wise for each objective i :

$$\delta_{0,i} = f_i(s_0, \delta_{init,i}) \quad (27)$$

The budget update rule is defined by $\delta' = \mathbf{g}(s, a, s', \delta)$, where $\mathbf{g} : S \times A \times S \times (\mathbb{R}^+)^N \rightarrow (\mathbb{R}^+)^N$. For independent constraints, this update is applied element-wise using the scalar update function g_i for each cost component:

$$\delta'_i = g_i(s, a, s', \delta_i) \quad (28)$$

Training Considerations We learn N independent cost-critics $\{Q_{C_i}^*, V_{C_i}^*\}_{i=1}^N$, one for each cost type. Since the persistent safety sets are computed independently of the policy, these critics can be trained in parallel. During the policy learning phase, we sample a budget vector δ such that $\delta_i \sim \mathcal{U}_{[Q_{C_i}^*(s,a), \delta_{max,i}]}$ for all i , ensuring the augmented transition remains within the intersection of all persistent safety sets.

B Additional Experiments

In additional experiments, we: **(1)** main results for both stochastic and deterministic approaches; **(2)** include an additional comparison with algorithms that are not adaptive to different cost budgets; **(3)** more details on the real-world maritime navigation experiment; **(4)** provide an ablation study on the expectile parameters for reward and cost (τ_R, τ_C), the temperature parameter β of IQL instantiation and the number of budget samples n used during training; **(5)** evaluate the quality of the learned feasible action set; **(6)** compare our results with the best policy obtained by LSPC to address the discrepancy discussed in Section C.6.

C Extended Related Work

Constrained Markov decision processes (CMDPs) (Altman 2021) are among the most widely adopted frameworks for safe RL. Numerous methods have been proposed to address the CMDP setting in offline RL. A simple approach is behavior cloning using only safe trajectories (Liu et al. 2024); CDT (Liu et al. 2023) extends the Decision Transformer (Chen et al. 2021) to handle action constraints. The DSRL benchmark (Liu et al. 2024) provides standardized datasets, benchmarks, and implementations. BCQ-Lagrangian (Liu et al. 2024) employs a Lagrangian approach to solve constrained problems; however, this method suffers from instability due to the difficulty of tuning the Lagrange multiplier, as it jointly optimizes both reward and cost objectives.

The COptiDICE algorithm (Lee et al. 2022) tackles the offline constrained setting via distribution correction estimation (DICE). Constrained Penalized Q-learning (CPQ) (Xu, Zhan, and Zhu 2022) formulates the problem as a min-max objective, which also leads to optimization instability. Despite their theoretical motivation, these methods have not demonstrated strong performance in prior safe offline RL benchmarks (Liu et al. 2024). Recently proposed CAPS algorithm (Chemingui et al. 2025) learns multiple policies and switches between them based on the remaining cost budget.

Recent work (Koirala et al. 2025) learns a variational autoencoder (VAE) (Kingma, Welling et al. 2019) to approximate the most conservative policy, and then trains a separate policy in the VAE’s latent space to maximize the reward. (Guo et al. 2025) improves upon this by conditioning the VAE on the remaining budget and sampling from it during training. Both approaches utilize variational autoencoders to learn generative models as a pre-training step, which incurs significant computational overhead.

	CDT		CAPS		CCAC		LSPC		BCRL (Ours)	
	reward \uparrow	cost \downarrow	reward \uparrow	cost \downarrow	reward \uparrow	cost \downarrow	reward \uparrow	cost \downarrow	reward \uparrow	cost \downarrow
PointButton1	0.53 \pm 0.01	1.68 \pm 0.13	0.04 \pm 0.15	0.58 \pm 1.42	0.68 \pm 0.14	4.31 \pm 3.20	0.09 \pm 0.20	0.69 \pm 1.03	0.07 \pm 0.18	0.79 \pm 2.10
PointButton2	0.46 \pm 0.01	1.57 \pm 0.10	0.12 \pm 0.20	0.96 \pm 2.35	0.63 \pm 0.11	4.82 \pm 3.61	0.19 \pm 0.21	1.39 \pm 2.53	0.12 \pm 0.22	0.81 \pm 1.36
PointCircle1	0.59 \pm 0.00	0.69 \pm 0.04	0.50 \pm 0.12	0.68 \pm 1.51	0.58 \pm 0.13	2.22 \pm 1.05	0.56 \pm 0.35	3.49 \pm 3.55	0.55 \pm 0.17	0.86 \pm 0.21
PointCircle2	0.64 \pm 0.01	1.05 \pm 0.08	0.51 \pm 0.21	0.76 \pm 0.47	0.18 \pm 0.50	1.42 \pm 1.09	0.67 \pm 0.24	4.18 \pm 4.56	0.58 \pm 0.10	0.74 \pm 0.34
PointGoal1	0.69 \pm 0.02	1.12 \pm 0.07	0.46 \pm 0.28	0.63 \pm 0.81	0.55 \pm 0.26	1.88 \pm 1.72	0.26 \pm 0.27	0.23 \pm 0.45	0.56 \pm 0.25	0.70 \pm 0.65
PointGoal2	0.59 \pm 0.03	1.34 \pm 0.05	0.34 \pm 0.23	0.80 \pm 0.74	0.41 \pm 0.36	3.60 \pm 3.37	0.23 \pm 0.24	0.50 \pm 0.79	0.38 \pm 0.21	0.77 \pm 0.68
PointPush1	0.24 \pm 0.02	0.48 \pm 0.05	0.15 \pm 0.17	0.33 \pm 0.66	0.02 \pm 0.33	1.42 \pm 5.37	0.14 \pm 0.18	0.37 \pm 0.77	0.14 \pm 0.16	0.47 \pm 0.79
PointPush2	0.21 \pm 0.04	0.65 \pm 0.03	0.12 \pm 0.19	0.60 \pm 1.12	-0.18 \pm 0.66	1.00 \pm 1.70	0.12 \pm 0.17	0.80 \pm 2.65	0.14 \pm 0.18	0.71 \pm 1.11
CarButton1	0.21 \pm 0.02	1.60 \pm 0.12	-0.02 \pm 0.17	0.26 \pm 0.53	0.45 \pm 0.26	11.31 \pm 8.91	-0.03 \pm 0.23	0.59 \pm 1.42	-0.06 \pm 0.18	0.34 \pm 0.76
CarButton2	0.13 \pm 0.01	1.58 \pm 0.02	-0.07 \pm 0.18	0.59 \pm 2.07	0.53 \pm 0.26	9.82 \pm 9.00	-0.13 \pm 0.28	0.93 \pm 2.06	-0.20 \pm 0.26	0.27 \pm 0.62
CarCircle1	0.60 \pm 0.01	1.73 \pm 0.04	0.55 \pm 0.16	1.54 \pm 1.63	0.49 \pm 0.14	5.13 \pm 3.53	0.46 \pm 0.25	1.86 \pm 3.14	0.50 \pm 0.12	0.48 \pm 0.43
CarCircle2	0.66 \pm 0.00	2.53 \pm 0.03	0.50 \pm 0.18	1.56 \pm 2.32	0.54 \pm 0.08	2.75 \pm 4.36	0.43 \pm 0.27	2.40 \pm 4.55	0.48 \pm 0.15	0.44 \pm 0.48
CarGoal1	0.66 \pm 0.01	1.21 \pm 0.17	0.32 \pm 0.26	0.33 \pm 0.53	0.84 \pm 0.08	1.81 \pm 1.91	0.27 \pm 0.26	0.24 \pm 0.44	0.43 \pm 0.27	0.43 \pm 0.58
CarGoal2	0.48 \pm 0.01	1.25 \pm 0.14	0.16 \pm 0.21	0.71 \pm 1.91	0.90 \pm 0.12	5.53 \pm 5.01	0.16 \pm 0.21	0.41 \pm 0.77	0.19 \pm 0.20	0.47 \pm 0.92
CarPush1	0.31 \pm 0.01	0.40 \pm 0.10	0.19 \pm 0.13	0.34 \pm 1.09	-0.12 \pm 0.70	0.59 \pm 0.97	0.18 \pm 0.15	0.41 \pm 1.29	0.19 \pm 0.14	0.24 \pm 0.74
CarPush2	0.19 \pm 0.01	1.30 \pm 0.16	0.05 \pm 0.14	0.71 \pm 1.66	0.12 \pm 0.31	6.06 \pm 9.53	0.07 \pm 0.15	0.80 \pm 1.41	0.05 \pm 0.17	0.52 \pm 1.07
SwimmerVelocity	0.66 \pm 0.01	0.96 \pm 0.08	0.44 \pm 0.22	1.66 \pm 2.37	-0.08 \pm 0.02	0.00 \pm 0.01	0.46 \pm 0.21	1.28 \pm 2.60	0.49 \pm 0.18	0.99 \pm 0.37
HopperVelocity	0.63 \pm 0.06	0.61 \pm 0.08	0.44 \pm 0.26	0.75 \pm 0.83	0.46 \pm 0.38	0.50 \pm 0.55	0.21 \pm 0.04	1.25 \pm 1.20	0.66 \pm 0.23	0.80 \pm 0.35
HalfCheetahVelocity	1.00 \pm 0.01	0.01 \pm 0.01	0.94 \pm 0.04	0.77 \pm 0.13	0.94 \pm 0.04	0.94 \pm 0.07	0.97 \pm 0.02	1.00 \pm 1.04	0.93 \pm 0.07	0.62 \pm 0.27
Walker2dVelocity	0.78 \pm 0.09	0.06 \pm 0.34	0.80 \pm 0.04	0.70 \pm 0.51	0.17 \pm 0.28	1.08 \pm 1.90	0.79 \pm 0.01	0.17 \pm 0.24	0.79 \pm 0.06	0.14 \pm 0.35
AntVelocity	0.98 \pm 0.00	0.39 \pm 0.12	0.95 \pm 0.04	0.64 \pm 0.21	0.51 \pm 0.41	0.59 \pm 0.34	0.97 \pm 0.05	0.14 \pm 0.15	0.97 \pm 0.03	0.34 \pm 0.14
SafetyGym Average (21 tasks)	0.54 \pm 0.21	1.06 \pm 0.59	0.36 \pm 0.34	0.76 \pm 1.43	0.41 \pm 0.46	3.18 \pm 5.24	0.34 \pm 0.19	1.10 \pm 1.75	0.38 \pm 0.17	0.57 \pm 0.68
BallRun	0.39 \pm 0.09	1.16 \pm 0.19	0.18 \pm 0.09	0.94 \pm 0.73	0.40 \pm 0.12	0.84 \pm 0.31	0.15 \pm 0.01	0.00 \pm 0.00	0.20 \pm 0.02	0.06 \pm 0.10
CarRun	0.99 \pm 0.01	0.65 \pm 0.31	0.97 \pm 0.01	0.23 \pm 0.25	0.97 \pm 0.04	0.68 \pm 0.22	0.98 \pm 0.01	0.84 \pm 1.04	0.98 \pm 0.01	0.98 \pm 0.72
DroneRun	0.63 \pm 0.04	0.79 \pm 0.68	0.45 \pm 0.10	2.91 \pm 4.46	0.46 \pm 0.18	4.36 \pm 4.32	0.59 \pm 0.06	0.93 \pm 1.51	0.58 \pm 0.03	0.54 \pm 0.91
AntRun	0.72 \pm 0.04	0.91 \pm 0.42	0.61 \pm 0.13	0.78 \pm 0.59	0.12 \pm 0.09	0.04 \pm 0.08	0.66 \pm 0.13	1.43 \pm 1.25	0.68 \pm 0.11	0.95 \pm 0.29
BallCircle	0.77 \pm 0.06	1.07 \pm 0.27	0.69 \pm 0.10	0.59 \pm 0.23	0.78 \pm 0.05	0.46 \pm 0.31	0.62 \pm 0.28	1.17 \pm 1.95	0.69 \pm 0.11	0.97 \pm 0.27
CarCircle	0.75 \pm 0.06	0.95 \pm 0.61	0.70 \pm 0.10	0.66 \pm 0.27	0.72 \pm 0.04	0.77 \pm 0.44	0.78 \pm 0.12	1.88 \pm 3.23	0.53 \pm 0.17	0.51 \pm 0.51
DroneCircle	0.63 \pm 0.07	0.98 \pm 0.27	0.55 \pm 0.06	0.65 \pm 0.29	0.29 \pm 0.27	0.63 \pm 0.70	0.60 \pm 0.02	1.31 \pm 0.86	0.42 \pm 0.12	0.52 \pm 0.32
AntCircle	0.54 \pm 0.20	1.78 \pm 4.33	0.37 \pm 0.18	0.15 \pm 0.25	0.61 \pm 0.14	0.75 \pm 0.90	0.44 \pm 0.14	0.53 \pm 0.93	0.56 \pm 0.17	0.79 \pm 0.60
BulletGym Average (8 tasks)	0.68 \pm 0.19	1.04 \pm 1.65	0.57 \pm 0.25	0.86 \pm 1.82	0.54 \pm 0.30	1.07 \pm 2.04	0.60 \pm 0.10	1.01 \pm 1.35	0.58 \pm 0.09	0.67 \pm 0.46
easysparse	0.17 \pm 0.14	0.23 \pm 0.32	0.12 \pm 0.20	0.37 \pm 0.43	-0.06 \pm 0.00	0.10 \pm 0.05	0.79 \pm 0.14	1.34 \pm 1.43	0.70 \pm 0.19	0.94 \pm 0.17
easymean	0.45 \pm 0.11	0.54 \pm 0.55	0.02 \pm 0.07	0.21 \pm 0.23	-0.06 \pm 0.01	0.07 \pm 0.08	0.82 \pm 0.06	1.33 \pm 0.86	0.73 \pm 0.17	0.94 \pm 0.13
easydense	0.32 \pm 0.18	0.62 \pm 0.43	0.11 \pm 0.15	0.16 \pm 0.17	-0.06 \pm 0.00	0.07 \pm 0.04	0.84 \pm 0.10	1.88 \pm 1.20	0.70 \pm 0.17	0.90 \pm 0.16
mediumsparse	0.87 \pm 0.11	1.10 \pm 0.26	0.59 \pm 0.36	0.74 \pm 0.97	-0.08 \pm 0.00	0.07 \pm 0.04	0.97 \pm 0.02	1.24 \pm 0.68	0.94 \pm 0.07	0.82 \pm 0.32
mediummean	0.45 \pm 0.39	0.75 \pm 0.83	0.66 \pm 0.35	0.90 \pm 0.89	-0.07 \pm 0.01	0.02 \pm 0.03	0.93 \pm 0.12	0.78 \pm 0.51	0.92 \pm 0.11	0.77 \pm 0.16
mediumdense	0.88 \pm 0.12	2.41 \pm 0.71	0.75 \pm 0.29	0.65 \pm 0.57	-0.08 \pm 0.00	0.06 \pm 0.03	0.82 \pm 0.30	1.07 \pm 0.71	0.78 \pm 0.28	0.68 \pm 0.31
hardsparse	0.25 \pm 0.08	0.41 \pm 0.33	0.45 \pm 0.15	0.75 \pm 0.56	-0.05 \pm 0.00	0.07 \pm 0.04	0.54 \pm 0.09	0.91 \pm 0.51	0.49 \pm 0.13	0.76 \pm 0.44
hardmean	0.33 \pm 0.21	0.97 \pm 0.31	0.29 \pm 0.13	0.28 \pm 0.31	-0.05 \pm 0.00	0.06 \pm 0.03	0.48 \pm 0.14	1.16 \pm 1.19	0.46 \pm 0.15	0.84 \pm 0.54
harddense	0.08 \pm 0.15	0.21 \pm 0.42	0.36 \pm 0.18	0.66 \pm 0.92	-0.03 \pm 0.01	0.11 \pm 0.08	0.47 \pm 0.19	1.43 \pm 0.93	0.44 \pm 0.17	0.63 \pm 0.24
MetaDrive Average (9 tasks)	0.42 \pm 0.31	0.80 \pm 0.61	0.38 \pm 0.34	0.54 \pm 0.69	-0.06 \pm 0.02	0.07 \pm 0.06	0.74 \pm 0.13	1.24 \pm 0.89	0.69 \pm 0.16	0.81 \pm 0.27

Table 3: **Results for normalized cost and normalized reward:** \uparrow indicates that a higher value is better, while \downarrow indicates that a lower value is preferable. **Bold** text denotes safe policies, gray indicates unsafe policies, and **blue** highlights the highest reward among the safe policies for each task. Each result is obtained by running three random seeds across three distinct cost thresholds and evaluating over 20 episodes.

Hamilton-Jacobi (HJ) reachable sets are useful for safety verification and policy supervision (Ganai, Gao, and Herbert 2024). In RL, feasible sets depend on the policy and change during training, causing instability. RCRL (Yu et al. 2022) uses a Lagrangian approach, while FISOR (Zheng et al. 2024) enforces hard constraints independently of the policy. Our method conditions feasibility on discounted future costs, enabling policy-independent estimation while handling cumulative soft constraints in CMDPs.

A related approach is Saute RL (Sootla et al. 2022), which enforces hard per-step constraints to satisfy the total cost limit. Instead of estimating future costs to select feasible actions, it labels timesteps by cumulative cost and requires an online RL setting to track the remaining budget during rollouts. In contrast, our approach prunes unsafe actions offline without requiring online samples.

C.1 Main Results with Stochastic and Deterministic Versions of Our Algorithm

In Table 4, we present results for both the stochastic and deterministic versions of our algorithm, shown side by side with other baselines. The main table in the paper reports results only for the default configuration (either the stochastic or deterministic variant, depending on the domain), while this section provides a detailed comparison of both. The results indicate that the stochastic version performs better in *SafetyGym* and *Bullet-SafetyGym*—domains with inherently stochastic dynamics—whereas the deterministic version achieves superior performance in *MetaDrive*, which features deterministic transitions.

	CDT		CAPS(IQL)		CCAC		LSPC-Final (Our-Run)		BCRL -Deterministic		BCRL -Stochastic	
	reward \uparrow	cost \downarrow	reward \uparrow	cost \downarrow	reward \uparrow	cost \downarrow	reward \uparrow	cost \downarrow	reward \uparrow	cost \downarrow	reward \uparrow	cost \downarrow
PointButton1	0.53 \pm 0.01	1.68 \pm 0.13	0.04 \pm 0.15	0.58 \pm 1.42	0.68 \pm 0.14	4.31 \pm 3.20	0.09 \pm 0.20	0.69 \pm 1.03	0.16 \pm 0.20	0.97 \pm 1.33	0.07 \pm 0.18	0.79 \pm 2.10
PointButton2	0.46 \pm 0.01	1.57 \pm 0.10	0.12 \pm 0.20	0.96 \pm 2.35	0.63 \pm 0.11	4.82 \pm 3.61	0.19 \pm 0.21	1.39 \pm 2.53	0.14 \pm 0.21	0.72 \pm 0.84	0.12 \pm 0.22	0.81 \pm 1.36
PointCircle1	0.59 \pm 0.00	0.69 \pm 0.04	0.50 \pm 0.12	0.68 \pm 1.51	0.58 \pm 0.13	2.22 \pm 1.05	0.56 \pm 0.35	3.49 \pm 3.55	0.47 \pm 0.10	0.78 \pm 0.87	0.55 \pm 0.17	0.86 \pm 0.21
PointCircle2	0.64 \pm 0.01	1.05 \pm 0.08	0.51 \pm 0.21	0.76 \pm 0.47	0.18 \pm 0.50	1.42 \pm 1.09	0.67 \pm 0.24	4.18 \pm 4.56	0.45 \pm 0.18	0.76 \pm 0.41	0.58 \pm 0.10	0.74 \pm 0.34
PointGoal1	0.69 \pm 0.02	1.12 \pm 0.07	0.46 \pm 0.28	0.63 \pm 0.81	0.55 \pm 0.26	1.88 \pm 1.72	0.26 \pm 0.27	0.23 \pm 0.45	0.61 \pm 0.21	0.88 \pm 0.65	0.56 \pm 0.25	0.70 \pm 0.65
PointGoal2	0.59 \pm 0.03	1.34 \pm 0.05	0.34 \pm 0.23	0.80 \pm 0.74	0.41 \pm 0.36	3.60 \pm 3.37	0.23 \pm 0.24	0.50 \pm 0.79	0.38 \pm 0.19	0.99 \pm 0.49	0.38 \pm 0.21	0.77 \pm 0.68
PointPush1	0.24 \pm 0.02	0.48 \pm 0.05	0.15 \pm 0.17	0.33 \pm 0.66	0.02 \pm 0.33	1.42 \pm 5.37	0.14 \pm 0.18	0.37 \pm 0.77	0.19 \pm 0.16	0.45 \pm 0.65	0.14 \pm 0.16	0.47 \pm 0.79
PointPush2	0.21 \pm 0.04	0.65 \pm 0.03	0.12 \pm 0.19	0.60 \pm 1.12	-0.18 \pm 0.66	1.00 \pm 1.70	0.12 \pm 0.17	0.80 \pm 2.65	0.12 \pm 0.19	0.88 \pm 2.85	0.14 \pm 0.18	0.71 \pm 1.11
CarButton1	0.21 \pm 0.02	1.60 \pm 0.12	-0.02 \pm 0.17	0.26 \pm 0.53	0.45 \pm 0.26	11.31 \pm 8.91	-0.03 \pm 0.23	0.59 \pm 1.42	0.04 \pm 0.17	0.62 \pm 0.68	-0.06 \pm 0.18	0.34 \pm 0.76
CarButton2	0.13 \pm 0.01	1.58 \pm 0.02	-0.07 \pm 0.18	0.59 \pm 2.07	0.53 \pm 0.26	9.82 \pm 9.00	-0.13 \pm 0.28	0.93 \pm 2.06	-0.16 \pm 0.25	0.36 \pm 0.51	-0.20 \pm 0.26	0.27 \pm 0.62
CarCircle1	0.60 \pm 0.01	1.73 \pm 0.04	0.55 \pm 0.16	1.54 \pm 1.63	0.49 \pm 0.14	5.13 \pm 3.53	0.46 \pm 0.25	1.86 \pm 3.14	0.37 \pm 0.16	0.54 \pm 0.55	0.50 \pm 0.12	0.48 \pm 0.43
CarCircle2	0.66 \pm 0.00	2.53 \pm 0.03	0.50 \pm 0.18	1.56 \pm 2.32	0.54 \pm 0.08	2.75 \pm 4.36	0.43 \pm 0.27	2.40 \pm 4.55	0.43 \pm 0.18	0.54 \pm 0.72	0.48 \pm 0.15	0.44 \pm 0.48
CarGoal1	0.66 \pm 0.01	1.21 \pm 0.17	0.32 \pm 0.26	0.33 \pm 0.53	0.84 \pm 0.08	1.81 \pm 1.91	0.27 \pm 0.26	0.24 \pm 0.44	0.49 \pm 0.22	0.64 \pm 0.69	0.43 \pm 0.27	0.43 \pm 0.58
CarGoal2	0.48 \pm 0.01	1.25 \pm 0.14	0.16 \pm 0.21	0.71 \pm 1.91	0.90 \pm 0.12	5.53 \pm 5.01	0.16 \pm 0.21	0.41 \pm 0.77	0.25 \pm 0.23	0.89 \pm 1.23	0.19 \pm 0.20	0.47 \pm 0.92
CarPush1	0.31 \pm 0.01	0.40 \pm 0.10	0.19 \pm 0.13	0.34 \pm 1.09	-0.12 \pm 0.70	0.59 \pm 0.97	0.18 \pm 0.15	0.41 \pm 1.29	0.20 \pm 0.12	0.25 \pm 0.50	0.19 \pm 0.14	0.24 \pm 0.74
CarPush2	0.19 \pm 0.01	1.30 \pm 0.16	0.05 \pm 0.14	0.71 \pm 1.66	0.12 \pm 0.31	6.06 \pm 9.53	0.07 \pm 0.15	0.80 \pm 1.41	0.08 \pm 0.15	0.53 \pm 0.75	0.05 \pm 0.17	0.52 \pm 1.07
SwimmerVelocity	0.66 \pm 0.01	0.96 \pm 0.08	0.44 \pm 0.22	1.66 \pm 2.37	-0.08 \pm 0.02	0.00 \pm 0.01	0.46 \pm 0.21	1.28 \pm 2.60	0.38 \pm 0.20	0.93 \pm 0.33	0.49 \pm 0.18	0.99 \pm 0.37
HopperVelocity	0.63 \pm 0.06	0.61 \pm 0.08	0.44 \pm 0.26	0.75 \pm 0.83	0.46 \pm 0.38	0.50 \pm 0.55	0.21 \pm 0.04	1.25 \pm 1.20	0.32 \pm 0.22	0.51 \pm 0.76	0.66 \pm 0.23	0.80 \pm 0.30
HalfCheetahVelocity	1.00 \pm 0.01	0.01 \pm 0.01	0.94 \pm 0.04	0.77 \pm 0.13	0.94 \pm 0.04	0.94 \pm 0.07	0.97 \pm 0.02	1.00 \pm 0.04	0.99 \pm 0.01	0.98 \pm 0.03	0.93 \pm 0.07	0.62 \pm 0.27
Walker2dVelocity	0.78 \pm 0.09	0.06 \pm 0.34	0.80 \pm 0.04	0.70 \pm 0.51	0.17 \pm 0.28	1.08 \pm 1.90	0.79 \pm 0.01	0.17 \pm 0.24	0.77 \pm 0.02	0.08 \pm 0.23	0.79 \pm 0.06	0.14 \pm 0.35
AntVelocity	0.98 \pm 0.00	0.39 \pm 0.12	0.95 \pm 0.04	0.64 \pm 0.21	0.51 \pm 0.41	0.59 \pm 0.34	0.97 \pm 0.05	0.14 \pm 0.15	0.98 \pm 0.05	0.42 \pm 0.24	0.97 \pm 0.03	0.34 \pm 0.14
SafetyGym Average	0.54 \pm 0.21	1.06 \pm 0.59	0.36 \pm 0.34	0.76 \pm 1.43	0.41 \pm 0.46	3.18 \pm 5.24	0.34 \pm 0.19	1.10 \pm 1.75	0.36 \pm 0.16	0.65 \pm 0.73	0.38 \pm 0.17	0.57 \pm 0.68
BallRun	0.39 \pm 0.09	1.16 \pm 0.19	0.18 \pm 0.09	0.94 \pm 0.73	0.40 \pm 0.12	0.84 \pm 0.31	0.15 \pm 0.01	0.00 \pm 0.00	0.22 \pm 0.13	0.87 \pm 1.35	0.20 \pm 0.02	0.06 \pm 0.10
CarRun	0.99 \pm 0.01	0.65 \pm 0.31	0.97 \pm 0.01	0.23 \pm 0.25	0.97 \pm 0.04	0.68 \pm 0.22	0.98 \pm 0.01	0.84 \pm 1.04	0.99 \pm 0.01	0.34 \pm 0.29	0.98 \pm 0.01	0.98 \pm 0.72
DroneRun	0.63 \pm 0.04	0.79 \pm 0.68	0.45 \pm 0.10	2.91 \pm 4.46	0.46 \pm 0.18	4.36 \pm 4.32	0.59 \pm 0.06	0.93 \pm 1.51	0.55 \pm 0.04	0.86 \pm 1.86	0.58 \pm 0.03	0.54 \pm 0.91
AntRun	0.72 \pm 0.04	0.91 \pm 0.42	0.61 \pm 0.13	0.78 \pm 0.59	0.12 \pm 0.09	0.04 \pm 0.08	0.66 \pm 0.13	1.43 \pm 1.25	0.57 \pm 0.14	0.61 \pm 0.34	0.68 \pm 0.11	0.95 \pm 0.29
BallCircle	0.77 \pm 0.06	1.07 \pm 0.27	0.69 \pm 0.10	0.59 \pm 0.23	0.78 \pm 0.05	0.46 \pm 0.31	0.62 \pm 0.28	1.17 \pm 1.95	0.59 \pm 0.12	0.86 \pm 0.15	0.69 \pm 0.11	0.97 \pm 0.27
CarCircle	0.75 \pm 0.06	0.95 \pm 0.61	0.70 \pm 0.10	0.66 \pm 0.27	0.72 \pm 0.04	0.77 \pm 0.44	0.78 \pm 0.12	1.88 \pm 3.23	0.42 \pm 0.19	0.88 \pm 0.33	0.53 \pm 0.17	0.51 \pm 0.51
DroneCircle	0.63 \pm 0.07	0.98 \pm 0.27	0.55 \pm 0.06	0.65 \pm 0.29	0.29 \pm 0.27	0.63 \pm 0.70	0.60 \pm 0.02	1.31 \pm 0.86	0.41 \pm 0.10	0.75 \pm 0.31	0.42 \pm 0.12	0.52 \pm 0.32
AntCircle	0.54 \pm 0.20	1.78 \pm 4.33	0.37 \pm 0.18	0.15 \pm 0.25	0.61 \pm 0.14	0.75 \pm 0.90	0.44 \pm 0.14	0.53 \pm 0.93	0.40 \pm 0.16	0.59 \pm 1.33	0.56 \pm 0.17	0.79 \pm 0.60
BulletGym Average	0.68 \pm 0.19	1.04 \pm 1.65	0.57 \pm 0.25	0.86 \pm 1.82	0.54 \pm 0.30	1.07 \pm 2.04	0.60 \pm 0.10	1.01 \pm 1.35	0.52 \pm 0.11	0.72 \pm 0.75	0.58 \pm 0.09	0.67 \pm 0.46
easysparse	0.17 \pm 0.14	0.23 \pm 0.32	0.12 \pm 0.20	0.37 \pm 0.43	-0.06 \pm 0.00	0.10 \pm 0.05	0.79 \pm 0.14	1.34 \pm 1.43	0.70 \pm 0.19	0.94 \pm 0.17	0.38 \pm 0.13	0.41 \pm 0.65
easymeans	0.45 \pm 0.11	0.54 \pm 0.55	0.02 \pm 0.07	0.21 \pm 0.23	-0.06 \pm 0.01	0.07 \pm 0.08	0.82 \pm 0.06	1.33 \pm 0.86	0.73 \pm 0.17	0.94 \pm 0.13	0.39 \pm 0.26	0.95 \pm 1.91
easymean	0.32 \pm 0.18	0.62 \pm 0.43	0.11 \pm 0.15	0.16 \pm 0.17	-0.06 \pm 0.00	0.07 \pm 0.04	0.84 \pm 0.10	1.88 \pm 1.20	0.70 \pm 0.17	0.90 \pm 0.16	0.34 \pm 0.21	0.51 \pm 1.24
mediumsparse	0.87 \pm 0.11	1.10 \pm 0.26	0.59 \pm 0.36	0.74 \pm 0.97	-0.08 \pm 0.00	0.07 \pm 0.04	0.97 \pm 0.02	1.24 \pm 0.68	0.94 \pm 0.07	0.82 \pm 0.32	0.65 \pm 0.15	0.14 \pm 0.16
mediummean	0.45 \pm 0.39	0.75 \pm 0.83	0.66 \pm 0.35	0.90 \pm 0.89	-0.07 \pm 0.01	0.02 \pm 0.03	0.93 \pm 0.12	0.78 \pm 0.51	0.92 \pm 0.11	0.77 \pm 0.16	0.67 \pm 0.19	0.32 \pm 0.37
mediumdense	0.88 \pm 0.12	2.41 \pm 0.71	0.75 \pm 0.29	0.65 \pm 0.57	-0.08 \pm 0.00	0.06 \pm 0.03	0.82 \pm 0.30	1.07 \pm 0.71	0.78 \pm 0.28	0.68 \pm 0.31	0.78 \pm 0.19	0.36 \pm 0.28
hardsparse	0.25 \pm 0.08	0.41 \pm 0.33	0.45 \pm 0.15	0.75 \pm 0.56	-0.05 \pm 0.00	0.07 \pm 0.04	0.54 \pm 0.09	0.91 \pm 0.51	0.49 \pm 0.13	0.76 \pm 0.44	0.40 \pm 0.17	0.83 \pm 0.89
hardmean	0.33 \pm 0.21	0.97 \pm 0.31	0.29 \pm 0.13	0.28 \pm 0.31	-0.05 \pm 0.00	0.06 \pm 0.03	0.48 \pm 0.14	1.16 \pm 1.19	0.46 \pm 0.15	0.84 \pm 0.54	0.38 \pm 0.16	0.81 \pm 0.94
harddense	0.08 \pm 0.15	0.21 \pm 0.42	0.36 \pm 0.18	0.66 \pm 0.92	-0.03 \pm 0.01	0.11 \pm 0.08	0.47 \pm 0.19	1.43 \pm 0.93	0.44 \pm 0.17	0.63 \pm 0.24	0.29 \pm 0.16	0.38 \pm 0.69
MetaDrive Average	0.42 \pm 0.31	0.80 \pm 0.61	0.38 \pm 0.34	0.54 \pm 0.69	-0.06 \pm 0.02	0.07 \pm 0.06	0.74 \pm 0.13	1.24 \pm 0.89	0.69 \pm 0.16	0.81 \pm 0.27	0.48 \pm 0.18	0.52 \pm 0.79

Table 4: **Results for normalized cost and normalized reward:** \uparrow indicates that a higher value is better, while \downarrow indicates that a lower value is preferable. **Bold** text denotes safe policies, **gray** indicates unsafe policies, and **blue** highlights the highest reward among the safe policies for each task. Each result is obtained by running three random seeds across three distinct cost thresholds and evaluating over 20 episodes.

C.2 Comparison with Non-Adaptive Baselines

	BC-Safe		BCQ-Lag		COptiDICE		CPQ		BCRL (Ours)	
	reward \uparrow	cost \downarrow	reward \uparrow	cost \downarrow	reward \uparrow	cost \downarrow	reward \uparrow	cost \downarrow	reward \uparrow	cost \downarrow
PointButton1	0.06 \pm 0.04	0.52 \pm 0.21	0.24 \pm 0.04	1.73 \pm 1.11	0.13 \pm 0.02	1.35 \pm 0.91	0.69 \pm 0.05	3.20 \pm 1.57	0.07 \pm 0.18	0.79 \pm 2.10
PointButton2	0.16 \pm 0.04	1.10 \pm 0.84	0.40 \pm 0.03	2.66 \pm 1.47	0.15 \pm 0.03	1.51 \pm 0.96	0.58 \pm 0.07	4.30 \pm 2.35	0.12 \pm 0.22	0.81 \pm 1.36
PointCircle1	0.41 \pm 0.08	0.16 \pm 0.11	0.54 \pm 0.17	2.38 \pm 1.30	0.86 \pm 0.01	5.51 \pm 2.93	0.43 \pm 0.07	0.75 \pm 1.86	0.55 \pm 0.17	0.86 \pm 0.21
PointCircle2	0.48 \pm 0.08	0.99 \pm 0.35	0.66 \pm 0.13	2.60 \pm 0.71	0.85 \pm 0.01	8.61 \pm 4.62	0.24 \pm 0.40	3.58 \pm 3.09	0.58 \pm 0.10	0.74 \pm 0.34
PointGoal1	0.43 \pm 0.12	0.54 \pm 0.24	0.71 \pm 0.02	0.98 \pm 0.46	0.49 \pm 0.05	1.66 \pm 1.05	0.57 \pm 0.08	0.35 \pm 0.37	0.56 \pm 0.25	0.70 \pm 0.65
PointGoal2	0.29 \pm 0.09	0.78 \pm 0.27	0.67 \pm 0.06	3.18 \pm 1.79	0.38 \pm 0.03	1.92 \pm 1.15	0.40 \pm 0.15	1.31 \pm 0.71	0.38 \pm 0.21	0.77 \pm 0.68
PointPush1	0.13 \pm 0.05	0.43 \pm 0.29	0.33 \pm 0.04	0.86 \pm 0.45	0.13 \pm 0.02	0.83 \pm 0.52	0.20 \pm 0.08	0.83 \pm 0.44	0.14 \pm 0.16	0.47 \pm 0.79
PointPush2	0.11 \pm 0.04	0.80 \pm 0.59	0.23 \pm 0.03	0.99 \pm 0.57	0.02 \pm 0.07	1.18 \pm 0.74	0.11 \pm 0.14	1.04 \pm 0.61	0.14 \pm 0.18	0.71 \pm 1.11
CarButton1	0.07 \pm 0.03	0.85 \pm 0.39	0.04 \pm 0.05	1.63 \pm 0.59	-0.08 \pm 0.09	1.68 \pm 1.29	0.42 \pm 0.05	9.66 \pm 5.71	-0.06 \pm 0.18	0.34 \pm 0.76
CarButton2	-0.01 \pm 0.02	0.63 \pm 0.30	0.06 \pm 0.05	2.13 \pm 1.19	-0.07 \pm 0.06	1.59 \pm 1.10	0.37 \pm 0.11	12.51 \pm 8.54	-0.20 \pm 0.26	0.27 \pm 0.62
CarCircle1	0.37 \pm 0.10	1.38 \pm 0.44	0.73 \pm 0.02	5.25 \pm 2.76	0.70 \pm 0.02	5.72 \pm 3.04	0.02 \pm 0.15	2.29 \pm 2.13	0.50 \pm 0.12	0.48 \pm 0.43
CarCircle2	0.54 \pm 0.08	3.38 \pm 1.30	0.72 \pm 0.04	6.58 \pm 3.02	0.77 \pm 0.03	7.99 \pm 4.23	0.44 \pm 0.10	2.69 \pm 2.61	0.48 \pm 0.15	0.44 \pm 0.48
CarGoal1	0.24 \pm 0.08	0.28 \pm 0.11	0.47 \pm 0.05	0.78 \pm 0.50	0.35 \pm 0.06	0.54 \pm 0.33	0.79 \pm 0.07	1.42 \pm 0.81	0.43 \pm 0.27	0.43 \pm 0.58
CarGoal2	0.14 \pm 0.05	0.51 \pm 0.26	0.30 \pm 0.05	1.44 \pm 0.99	0.25 \pm 0.04	0.91 \pm 0.41	0.65 \pm 0.20	3.75 \pm 2.00	0.19 \pm 0.20	0.47 \pm 0.92
CarPush1	0.14 \pm 0.03	0.33 \pm 0.23	0.23 \pm 0.03	0.43 \pm 0.19	0.23 \pm 0.04	0.50 \pm 0.40	-0.03 \pm 0.24	0.95 \pm 0.53	0.19 \pm 0.14	0.24 \pm 0.74
CarPush2	0.05 \pm 0.02	0.45 \pm 0.19	0.15 \pm 0.02	1.38 \pm 0.68	0.09 \pm 0.02	1.07 \pm 0.69	0.24 \pm 0.06	4.25 \pm 2.44	0.05 \pm 0.17	0.52 \pm 1.07
SwimmerVelocity	0.51 \pm 0.20	1.07 \pm 0.07	0.48 \pm 0.33	6.58 \pm 3.95	0.63 \pm 0.06	7.58 \pm 1.77	0.13 \pm 0.06	2.66 \pm 0.96	0.49 \pm 0.18	0.99 \pm 0.37
HopperVelocity	0.36 \pm 0.13	0.67 \pm 0.27	0.78 \pm 0.09	5.02 \pm 3.43	0.13 \pm 0.06	1.51 \pm 1.54	0.14 \pm 0.09	2.11 \pm 2.29	0.66 \pm 0.23	0.80 \pm 0.35
HalfCheetahVelocity	0.88 \pm 0.03	0.54 \pm 0.63	1.05 \pm 0.07	18.21 \pm 8.29	0.65 \pm 0.01	0.00 \pm 0.00	0.29 \pm 0.14	0.74 \pm 0.19	0.93 \pm 0.07	0.62 \pm 0.37
Walker2dVelocity	0.79 \pm 0.05	0.04 \pm 0.32	0.79 \pm 0.01	0.17 \pm 0.06	0.12 \pm 0.01	0.74 \pm 0.07	0.04 \pm 0.05	0.21 \pm 0.09	0.79 \pm 0.06	0.14 \pm 0.35
AntVelocity	0.98 \pm 0.01	0.29 \pm 0.10	1.02 \pm 0.01	4.15 \pm 1.63	1.00 \pm 0.00	3.28 \pm 2.01	-1.01 \pm 0.00	0.00 \pm 0.00	0.97 \pm 0.03	0.34 \pm 0.14
SafetyGym Average	0.34 \pm 0.31	0.75 \pm 0.80	0.50 \pm 0.32	3.29 \pm 4.97	0.37 \pm 0.32	2.65 \pm 3.24	0.27 \pm 0.37	2.79 \pm 3.86	0.38 \pm 0.17	0.57 \pm 0.68
BallRun	0.27 \pm 0.14	1.46 \pm 0.39	0.76 \pm 0.01	3.91 \pm 0.35	0.59 \pm 0.00	3.52 \pm 0.00	0.22 \pm 0.00	1.27 \pm 0.12	0.20 \pm 0.02	0.06 \pm 0.10
CarRun	0.94 \pm 0.00	0.22 \pm 0.02	0.94 \pm 0.01	0.15 \pm 0.91	0.87 \pm 0.00	0.00 \pm 0.00	0.95 \pm 0.01	1.79 \pm 0.18	0.98 \pm 0.01	0.98 \pm 0.72
DroneRun	0.28 \pm 0.25	0.74 \pm 0.97	0.72 \pm 0.12	5.54 \pm 0.81	0.67 \pm 0.02	4.15 \pm 0.10	0.33 \pm 0.10	3.52 \pm 0.58	0.58 \pm 0.03	0.54 \pm 0.91
AntRun	0.65 \pm 0.15	1.09 \pm 0.84	0.76 \pm 0.07	5.11 \pm 2.39	0.61 \pm 0.01	0.94 \pm 0.69	0.03 \pm 0.02	0.02 \pm 0.09	0.68 \pm 0.11	0.95 \pm 0.29
BallCircle	0.52 \pm 0.08	0.65 \pm 0.17	0.69 \pm 0.11	2.36 \pm 1.04	0.70 \pm 0.04	2.61 \pm 0.79	0.64 \pm 0.01	0.76 \pm 0.00	0.69 \pm 0.11	0.97 \pm 0.27
CarCircle	0.50 \pm 0.22	0.84 \pm 0.67	0.63 \pm 0.19	1.89 \pm 1.37	0.49 \pm 0.05	3.14 \pm 2.98	0.71 \pm 0.02	0.33 \pm 0.00	0.53 \pm 0.17	0.51 \pm 0.51
DroneCircle	0.56 \pm 0.18	0.57 \pm 0.27	0.80 \pm 0.07	3.07 \pm 0.89	0.26 \pm 0.03	1.02 \pm 0.46	-0.22 \pm 0.05	1.28 \pm 0.97	0.42 \pm 0.12	0.52 \pm 0.32
AntCircle	0.40 \pm 0.16	0.96 \pm 2.67	0.58 \pm 0.25	2.87 \pm 3.08	0.17 \pm 0.10	5.04 \pm 6.70	-	-	0.56 \pm 0.17	0.79 \pm 0.60
BulletGym Average	0.52 \pm 0.27	0.82 \pm 1.27	0.74 \pm 0.25	3.11 \pm 3.55	0.55 \pm 0.24	2.55 \pm 3.62	0.33 \pm 0.29	1.12 \pm 1.85	0.58 \pm 0.09	0.67 \pm 0.46
easysparse	0.11 \pm 0.08	0.21 \pm 0.02	0.78 \pm 0.00	5.01 \pm 0.06	0.96 \pm 0.02	5.44 \pm 0.27	-0.06 \pm 0.00	0.07 \pm 0.02	0.70 \pm 0.19	0.94 \pm 0.17
easymeans	0.04 \pm 0.03	0.29 \pm 0.02	0.71 \pm 0.06	3.44 \pm 0.35	0.66 \pm 0.16	3.97 \pm 1.47	-0.07 \pm 0.00	0.07 \pm 0.01	0.73 \pm 0.17	0.94 \pm 0.13
easydense	0.11 \pm 0.07	0.14 \pm 0.01	0.26 \pm 0.00	0.47 \pm 0.01	0.50 \pm 0.10	2.54 \pm 0.53	-0.06 \pm 0.00	0.03 \pm 0.01	0.70 \pm 0.17	0.90 \pm 0.16
mediumsparse	0.33 \pm 0.34	0.30 \pm 0.32	0.44 \pm 0.00	1.16 \pm 0.02	0.71 \pm 0.37	2.49 \pm 1.90	-0.08 \pm 0.02	0.07 \pm 0.03	0.94 \pm 0.07	0.82 \pm 0.32
mediummean	0.31 \pm 0.06	0.21 \pm 0.00	0.78 \pm 0.12	1.53 \pm 0.21	0.76 \pm 0.34	2.05 \pm 0.92	-0.08 \pm 0.00	0.05 \pm 0.02	0.92 \pm 0.11	0.77 \pm 0.16
mediumdense	0.24 \pm 0.00	0.17 \pm 0.00	0.58 \pm 0.21	1.89 \pm 1.19	0.69 \pm 0.13	2.24 \pm 0.65	-0.07 \pm 0.00	0.07 \pm 0.01	0.78 \pm 0.28	0.68 \pm 0.31
hardsparse	0.17 \pm 0.05	3.25 \pm 0.10	0.50 \pm 0.04	1.02 \pm 0.05	0.37 \pm 0.10	2.05 \pm 0.27	-0.05 \pm 0.00	0.06 \pm 0.01	0.49 \pm 0.13	0.76 \pm 0.44
hardmean	0.13 \pm 0.00	0.40 \pm 0.00	0.47 \pm 0.13	2.56 \pm 0.72	0.32 \pm 0.19	2.47 \pm 2.00	-0.05 \pm 0.00	0.06 \pm 0.02	0.46 \pm 0.15	0.84 \pm 0.54
harddense	0.15 \pm 0.06	0.22 \pm 0.01	0.35 \pm 0.03	1.40 \pm 0.14	0.24 \pm 0.21	1.68 \pm 2.15	-0.04 \pm 0.01	0.08 \pm 0.01	0.44 \pm 0.17	0.63 \pm 0.24
MetaDrive Average	0.18 \pm 0.27	0.58 \pm 0.35	0.54 \pm 0.35	2.05 \pm 2.70	0.58 \pm 0.32	2.77 \pm 2.87	-0.06 \pm 0.01	0.06 \pm 0.04	0.69 \pm 0.16	0.81 \pm 0.27

Table 5: **Comparison with Non-Adaptive Baselines:** This table presents results similar to our main results table (Table 1), but includes additional baseline methods that do not generalize to varying cost budgets. The results for these baselines are taken from the DSRL benchmark (Liu et al. 2024).

neural network architecture.

Action Space In ShipNaviSim, the action space is a 3-dimensional continuous “delta” action space, represented as $\langle d_x, d_y, d_h \rangle$, corresponding to changes in x , y , and heading h between consecutive steps. The vessel’s speed at the next timestep is computed from the distance traveled, using $v_{t+1} = \sqrt{d_x^2 + d_y^2} / \delta T$ with a timestep of $\delta T = 10$ seconds. Because actions encode differences between consecutive states, a simple inverse-kinematics model can be used to infer actions directly from state-only trajectories in the dataset.

Evaluation Metrics We evaluate navigation behavior using several vessel-specific metrics that compare agent trajectories with human expert data.

Goal-Conditioned ADE (GC-ADE) GC-ADE measures the average 2D displacement error between the agent’s trajectory and the historical trajectory. For trajectories τ_m and τ_p of lengths T_m and T_p , the metric is computed over $\min(T_m, T_p)$ steps:

$$\text{GC-ADE} = \frac{1}{\min(T_m, T_p)} \sqrt{\sum_{t=1}^{\min(T_m, T_p)} (x_t^m - x_t^p)^2 + (y_t^m - y_t^p)^2}$$

Success Rate Success rate is defined as the percentage of episodes in which the ego vessel reaches its assigned goal, with success determined by entering a 200-meter radius around the goal.

Close-quarters Rate Close-quarters rate measures the proportion of timesteps in an episode where the ego vessel comes within

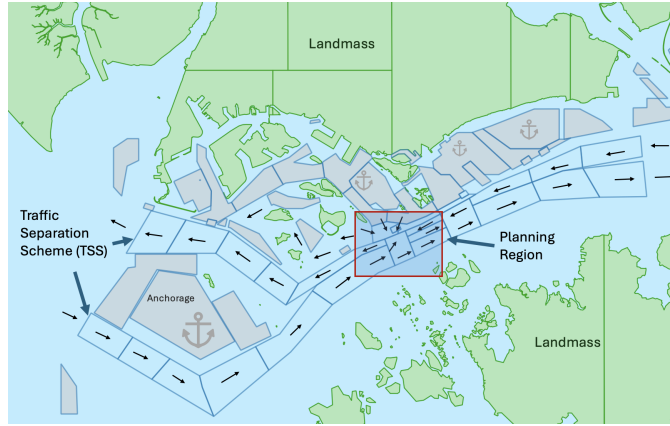


Figure 5: The red region is used as the environment area. The gray areas indicate anchorage zones, the green areas represent landmasses, and the arrows and regions with dark blue borders represent the Maritime Traffic Separation Scheme (TSS). The high density of crossing points in the red area makes it a more challenging region for navigation, providing a suitable setting for testing advanced planning techniques.

3 cable lengths (555 meters) of another vessel—a distance regarded by domain experts as a close-quarters situation. This metric serves as a coarse indicator of traffic density and potential navigational risk; it does not necessarily imply that a collision was imminent.

Reward. The reward function is defined as a sparse signal: the agent receives a reward of 100 only when it successfully reaches the goal. No intermediate rewards are provided, which encourages the agent to focus on completing the task while avoiding unsafe situations.

Cost. The cost function is defined to capture close-quarters situations. Specifically, for each transition, if the next state s' results in the agent coming too close to another vessel (i.e., a close-quarters scenario), the cost is set to $c(s, a) = 1$; otherwise, $c(s, a) = 0$. This formulation directly penalizes unsafe maneuvers and encourages the agent to maintain safe distances from other vessels throughout its trajectory.

C.4 Ablations on Key Hyperparameters

In our approach, the IQL instantiation is primarily governed by three hyperparameters: the expectile for training the cost critic (τ_C), the expectile for the reward critic (τ_R), and the policy extraction temperature associated with AWR (β). Among these, the expectile values are particularly important for performance, as also observed in the original IQL work (Kostrikov, Nair, and Levine 2022). A lower cost critic expectile ($\tau_C \leq 0.5$) encourages a more conservative cost estimate that prioritizes minimizing cost, and our experiments indicate that better results are achieved with smaller τ_C . Conversely, the reward critic expectile is chosen to be $\tau_R \geq 0.5$, aligning with the recommendations from the IQL paper (Kostrikov, Nair, and Levine 2022). Ablation results for these expectile values are presented in Table 6.

C.5 Feasible Action Set Analysis

In Figure 6 we present the percentage of feasible actions to evaluate how restrictive or inclusive our learned feasible action space is. Using the learned cost critic, we estimate the percentage of (s, a) pairs from the dataset that are feasible based on the remaining budget δ , given by $\frac{\sum_{(s,a) \in \mathcal{D}} \mathbb{I}[Q_C^*(s,a) \leq \delta]}{|\mathcal{D}|}$. If the remaining budget is ≥ 15 , almost all the samples become feasible for most of the environments. For example, CarPush1 and MataDrive-mediummean, feasibility reaches 99% by budget 5, and 65% of the actions become feasible in AntCircle. This indicates the feasible action set is not over-conservative.

Expectile τ_r	0.5		0.6		0.7	
	cost ↓	reward ↑	cost ↓	reward ↑	cost ↓	reward ↑
HopperVelocityGymnasium	0.83	0.79	0.80	0.66	0.85	0.60
PointPush1Gymnasium	0.40	0.17	0.46	0.14	0.34	0.17
PointPush2Gymnasium	0.66	0.12	0.71	0.14	0.68	0.12
SwimmerVelocityGymnasium	0.82	0.36	0.98	0.49	0.99	0.38
AntRun	0.95	0.68	1.00	0.69	0.98	0.68
BallRun	0.07	0.20	3.30	0.24	2.43	0.22
CarRun	0.98	0.98	0.30	0.98	0.26	0.98
DroneRun	0.54	0.58	2.75	0.66	0.66	0.60

Cost Expectile τ_c	0.2		0.3		0.4	
	cost ↓	reward ↑	cost ↓	reward ↑	cost ↓	reward ↑
HopperVelocityGymnasium	1.19	0.39	0.80	0.66	0.21	0.43
PointPush1Gymnasium	0.72	0.21	0.46	0.14	0.25	0.11
PointPush2Gymnasium	1.07	0.15	0.71	0.14	0.58	0.12
SwimmerVelocityGymnasium	2.19	0.30	0.98	0.49	1.19	0.57
AntRun	0.95	0.68	0.47	0.62	0.33	0.62
BallRun	0.07	0.20	3.09	0.06	3.79	0.01
CarRun	0.98	0.98	0.58	0.98	0.21	0.90
DroneRun	0.54	0.58	0.11	0.16	0.00	-0.01

Table 6: Ablation on the Reward Expectile τ_R Cost Expectile τ_C

C.6 Compare our results with the best policy obtained by LSPC

Table 7 reports results using the best policy selected during training. In the original LSPC (Koirala et al. 2025) work, policies were evaluated every 20k steps over a 1M-step training run, which allows selection of a high-performing policy but assumes access to a simulator—often unavailable in offline RL settings. To ensure a fair comparison, we reproduced this evaluation strategy for both our approach and LSPC, selecting and reporting the best-performing policy during training. As shown in the table, our method remains competitive under these conditions, with blue indicating the best results. All environments exhibit safe policies under this evaluation protocol.

C.7 Grid World Environment

Figure 7 shows the grid-world environment used for the results in Figure 3. The action space consists of moving left, right, up, or down. The transition probability of the intended movement p is the probability of moving in the chosen direction, with the remaining probability distributed among the other three actions. We vary p and the budget to evaluate our method.

C.8 Approximated Persistent Safety

In this section, we examine how sensitive our approach is to the quality of the learned persistent safety set. We approximate this set by learning the cost critic (cost-value function). In this experiment, we early-stop cost-critic training at 20%, 50%, 80%, and 100% of the training steps, then evaluate the results shown in Figure 8. The results show that reducing the cost-critic quality leads to slightly higher constraint violations, but the effect is minor.

D Implementation Details

D.1 Implementation Details CMDP

Given a CMDP, we first solve the MDP to minimize the budget and obtain solutions for V_C^* and Q_C^* . These solutions are then used to construct BAMDP. To keep the state space finite and discrete, we discretize the budget and add it as an additional dimension to the state space. The transition function is updated based on the BAMDP transition function \bar{T} . The budget update functions f, g are real-valued functions, which must be discretized to be compatible with the discrete budget, in that case we can round the real budget to the nearest budget-bin. States outside the persistent safety set \bar{S}_P are masked, and the action space is restricted to the support of Π_P . The resulting extended MDP can then be solved using a standard LP solver. In the policy extraction, we can only include the actions in the persistently safe actions $A_P(s, \delta)$. Also, we will learn the policy for states outside the persistent safety set $s \notin \bar{S}_P$ to minimize the cost in case the agent leaves the persistent state set \bar{S}_P , mainly because of the approximation errors caused by discretization.

Algorithm 2: Construction and LP Solution of the Extended MDP

Require: CMDP $\mathcal{M} := \langle S, A, T, r, c, \gamma, \mu_0, \delta_{\text{init}} \rangle$, budget update function g

- 1: Compute cost value functions V_C^* and Q_C^* by minimizing cost in \mathcal{M} (Standard LP formulation)
 - 2: Construct discrete budget space B via binning over $[0, \delta_{\text{max}}]$
 - 3: Modified state space of BDMDP $\bar{S} := S \times B$ and persistent state space $\bar{S}_P := \{(s, \delta) \in \bar{S} | V_C^*(s) \leq \delta\}$
 - 4: Define the persistent action space $A_P(s, \delta) := \{a \in A | Q_C^*(s, a) \leq \delta\} \quad \forall (s, \delta) \in \bar{S}$
 - 5: Define the extended transition function: $\bar{T}((s', \delta') | (s, \delta), a) := T(s' | s, a) \cdot \mathbf{1}_{\{\delta' = g(s, a, s', \delta)\}}$
 - 6: Solve the extended MDP via LP, only considering the persistent state set \bar{S}_P and persistent action set A_P to obtain Q_R^*
 - 7: Extract policy: $\pi(s, \delta) \leftarrow \begin{cases} \arg \max_{a \in A_P(s, \delta)} Q_R^*(s, a), & \text{if } s \in \bar{S}_P \\ \arg \min_a Q_C^*(s, a), & s \notin \bar{S}_P \end{cases}$
 - 8: **return** π
-

D.2 Implementation Details Offlien RL

In the main results, we include CDT, CAPS, LSPC, and CCAC as baselines. All baselines are evaluated using the same cost thresholds and trained with the same number of gradient steps (SafetyGym and BulletGym: 100k steps; MetaDrive: 200k steps) as proposed in the DSRL benchmark and the final policy is used for evaluation. Details are specified in Table 10. For baselines where standard deviation is not reported in the published paper (CAPS), or they are not tested on some DSRL instances (CCAC), we run them again using their author provided code and hyperparams. The CDT results are taken from the published paper as it is tested on all domains with standard deviations.

For LSPC, we use the official source code and hyper-parameters from the original authors (Koirala et al. 2025). The original work trained the model for 1M steps, evaluated policy every 20k steps, and reported the *best policy*'s results after 1M training steps. However, this training method is not standard, as during policy training, access to simulator is not assumed in standard DSRL baselines. To ensure a fair comparisons across all the methods, instead we train the LSPC model with the same number

Algorithm 3: BCRL: Execution (for finite horizon)

Input: environment Env , cost threshold δ_{mit} and maximum episode length of the environment H

$c \leftarrow 0$ ▷ Initialize total cost to zero
 $t \leftarrow 0$ ▷ Initialize total timesteps to zero
 $s \leftarrow Env.\text{reset}()$; $done \leftarrow \text{False}$

repeat

$\delta \leftarrow \frac{\delta_{\text{mit}} - c}{(1-\gamma)} \frac{1-\gamma^{H-t}}{H-t}$ ▷ Calculate the dynamic budget constraint to enforce based on the remaining steps and remaining budget for finite horizon tasks

$a \sim \pi((s, \delta))$
 $s', r(s, a), c(s, a), done \leftarrow Env.\text{step}(a)$
 $s \leftarrow s'$

until $done$

of gradient steps as the other baselines and report results from the final policy in the Main Paper Table 1. For completeness sake, we also compare the best policies of both LSPC and our method over 1M training in Table 7.

Our Algorithm Details Our algorithm was trained for the same number of gradient steps, using the exact hyperparameters listed in Table 10. These hyperparameters were selected through manual experimentation, guided by Bayesian hyperparameter search, over value ranges explored in the ablation study presented in the experimental section. The complete implementation of our algorithm is available in the Supplementary Material. Hyperparameters for different domains are presented in Table 10, and the training algorithm is detailed in Algorithm 1. Though our algorithm consists of three isolated loops (cost critic learning, reward critic learning, and policy extraction), since each loop depends only on its own previous steps, they can be implemented in a single loop with gradient updates. We follow this approach to keep things simple since it allow us to evaluate the policy while training.

Metrics. We use the standard metrics proposed in the DSRL benchmark (Liu et al. 2024), namely *normalized reward* and *normalized cost*. These are computed using the following formulas:

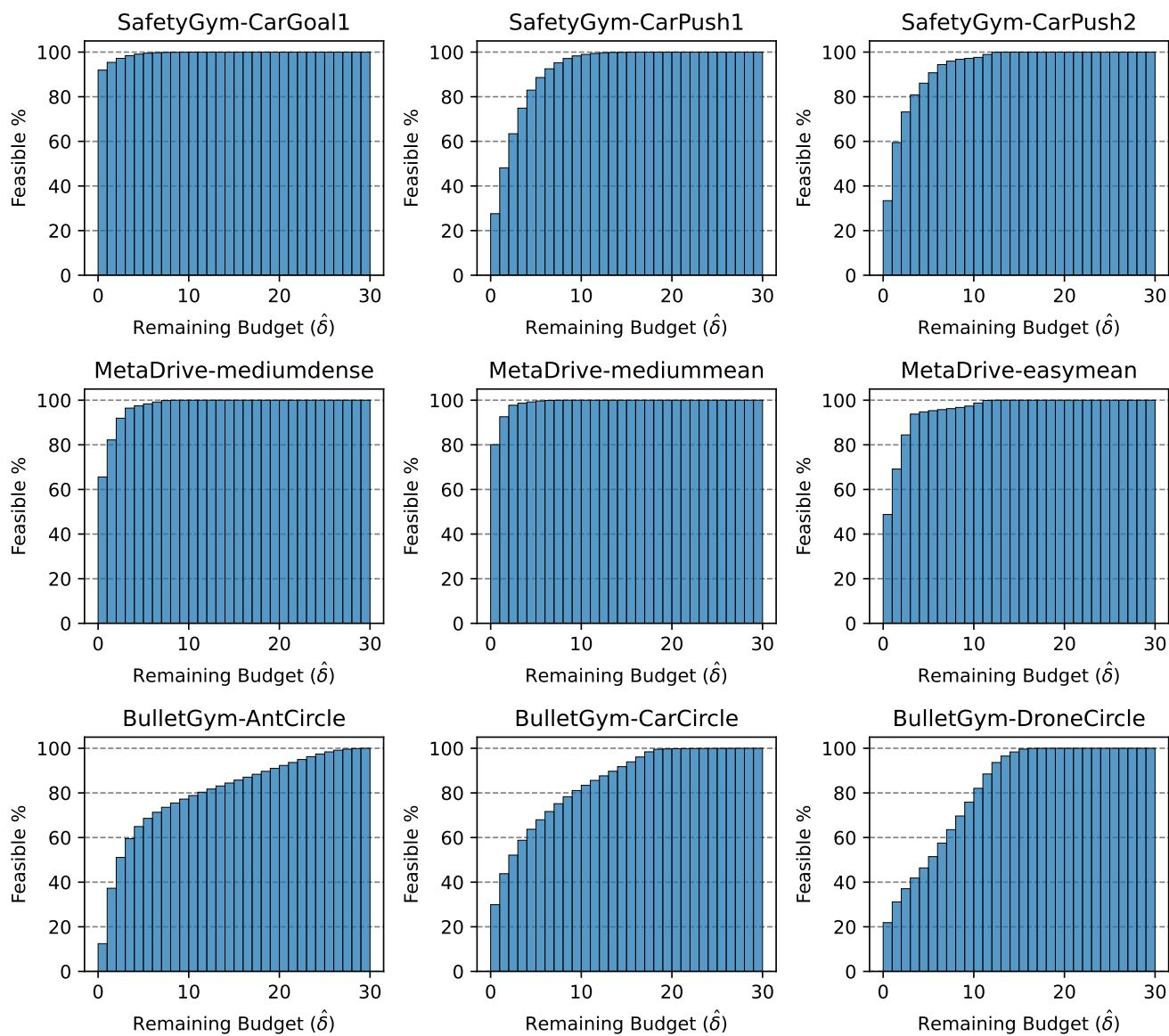
$$R_{\text{normalized}} = \frac{R_{\pi} - R_{\min}}{R_{\max} - R_{\min}}, \quad C_{\text{normalized}} = \frac{C_{\pi} - C_{\min}}{C_{\max} - C_{\min}} \quad (29)$$

Here, R_{\min} and R_{\max} denote the minimum and maximum empirical returns, respectively, while C_{\min} and C_{\max} denote the minimum and maximum empirical costs of the particular task.

Evaluation: The algorithm for evaluating a policy using the trained budget-conditioned policy is provided in Algorithm 3. Since the task is in-practice finite horizon, we adjust the cost budget based on the maximum horizon as in the Algorithm 3. It calculates the budget required based on the remaining steps and remaining budget. This idea was used in previous works (Chemingui et al. 2025).

Run Time. We benchmarked the training and evaluation time of our algorithm on a server equipped with an NVIDIA GeForce RTX 3090 GPU. The results are reported in Table 9. Our method completes in just a few minutes, offering a noticeable speed-up compared to several baseline methods, which may take 2–3 hours to train under identical hardware and conditions. While we acknowledge that runtime comparisons are inherently approximate, the results suggest that our approach has the potential for substantial improvements in efficiency.

Figure 6: Percentage of Feasible Action Samples:



Task	LSPC-Best-Policy		BCAP-Best-Policy(ours)	
	reward \uparrow	cost \downarrow	reward \uparrow	cost \downarrow
PointButton1	0.10\pm0.19	0.72\pm1.17	0.16\pm0.21	0.81\pm1.07
PointButton2	0.17\pm0.20	1.01\pm1.52	0.23\pm0.26	0.89\pm1.06
PointCircle1	0.32\pm0.18	0.01\pm0.07	0.47\pm0.19	0.97\pm0.84
PointCircle2	0.44\pm0.21	0.00\pm0.00	0.54\pm0.19	0.81\pm0.82
PointGoal1	0.41\pm0.31	0.46\pm0.76	0.68\pm0.17	0.98\pm0.93
PointGoal2	0.21\pm0.23	0.58\pm0.95	0.16\pm0.38	0.92\pm1.11
PointPush1	0.14\pm0.17	0.42\pm0.79	0.24\pm0.17	0.45\pm0.59
PointPush2	0.13\pm0.16	0.56\pm1.30	0.20\pm0.17	0.72\pm0.95
CarButton1	-0.05\pm0.19	0.58\pm1.48	0.07\pm0.15	0.70\pm1.05
CarButton2	-0.13\pm0.24	0.84\pm1.89	-0.07\pm0.25	0.72\pm1.23
CarCircle1	0.34\pm0.14	0.22\pm0.52	0.38\pm0.16	0.53\pm0.55
CarCircle2	0.36\pm0.21	0.59\pm1.49	0.51\pm0.16	0.98\pm1.02
CarGoal1	0.29\pm0.27	0.36\pm0.64	0.50\pm0.24	0.73\pm0.97
CarGoal2	0.15\pm0.21	0.53\pm1.20	0.30\pm0.22	0.89\pm1.00
CarPush1	0.20\pm0.13	0.29\pm0.73	0.26\pm0.14	0.39\pm0.94
CarPush2	0.09\pm0.16	0.66\pm1.09	0.13\pm0.16	0.73\pm1.00
SwimmerVelocity	0.56\pm0.13	0.26\pm0.63	0.31\pm0.25	0.86\pm1.88
HopperVelocity	0.24\pm0.02	0.34\pm0.39	0.72\pm0.16	0.61\pm0.45
HalfCheetahVelocity	0.99\pm0.02	0.59\pm0.73	0.96\pm0.02	0.87\pm0.85
Walker2dVelocity	0.80\pm0.05	0.29\pm0.45	0.80\pm0.01	0.06\pm0.16
AntVelocity	0.98\pm0.05	0.29\pm0.23	0.99\pm0.01	0.68\pm0.40
BallRun	0.21\pm0.03	0.00\pm0.00	0.19\pm0.23	0.32\pm0.67
CarRun	0.98\pm0.00	0.44\pm0.46	0.99\pm0.00	0.72\pm0.43
DroneRun	0.59\pm0.03	0.40\pm1.16	0.58\pm0.01	0.31\pm0.60
AntRun	0.43\pm0.13	0.48\pm0.49	0.72\pm0.01	0.59\pm0.42
BallCircle	0.49\pm0.16	0.04\pm0.09	0.76\pm0.05	0.93\pm0.43
CarCircle	0.73\pm0.03	0.13\pm0.32	0.72\pm0.05	0.68\pm0.62
DroneCircle	0.54\pm0.04	0.72\pm0.61	0.54\pm0.04	0.69\pm0.51
AntCircle	0.44\pm0.14	0.45\pm0.82	0.60\pm0.12	0.77\pm0.77
easysparse	0.72\pm0.00	0.54\pm0.29	0.70\pm0.19	0.94\pm0.17
easymean	0.72\pm0.01	0.53\pm0.29	0.73\pm0.17	0.94\pm0.13
easydense	0.71\pm0.02	0.53\pm0.29	0.70\pm0.17	0.90\pm0.16
mediumsparse	0.95\pm0.07	0.10\pm0.07	0.94\pm0.07	0.82\pm0.32
mediummean	0.91\pm0.11	0.44\pm0.29	0.92\pm0.11	0.77\pm0.16
mediumdense	0.90\pm0.12	0.37\pm0.35	0.78\pm0.28	0.68\pm0.31
hardsparse	0.53\pm0.10	0.46\pm0.29	0.49\pm0.13	0.76\pm0.44
hardmean	0.52\pm0.09	0.30\pm0.19	0.46\pm0.15	0.84\pm0.54
harddense	0.52\pm0.10	0.37\pm0.23	0.44\pm0.17	0.63\pm0.24

Table 7: Performance of the best policy evaluated during training.

task		% of cost critic learning			
		20%	50%	80%	100%
CarCircle1	reward	0.68	0.55	0.58	0.50
	cost	2.79	1.22	1.72	0.50
CarCircle2	reward	0.59	0.60	0.51	0.47
	cost	2.49	3.36	1.03	0.53
CarGoal1	reward	0.45	0.39	0.36	0.39
	cost	0.60	0.49	0.45	0.39
CarGoal2	reward	0.21	0.17	0.16	0.17
	cost	0.74	0.61	0.55	0.49
HalfCheetahVelocity	reward	0.97	0.94	0.92	0.92
	cost	0.70	0.64	0.77	0.63
HopperVelocity	reward	0.47	0.67	0.47	0.61
	cost	1.09	0.95	0.86	0.75

Table 8: Ablation by partially learning cost critic

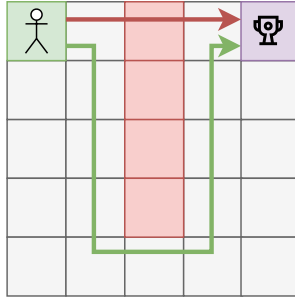


Figure 7: **Grid-World Environment:** The agent starts at the green cell and receives a reward of -1 per step. Reaching the target green cell terminates the episode. We vary the transition probability of the intended movement to make navigation more difficult and stochastic, resulting in a non-zero expected cost.

	BulletGym	SafetGym	MetaDrive
Average Training Time	7.1 minutes	8.5 minutes	18.4 minutes
Evaluation Time	1.1 minute	4.1 minutes	10.8 minutes
Training Steps	100k	100k	200k

Table 9: Average Training and evaluation time per instance (by evaluating on 3 distinct cost thresholds, 20 episodes)

Hyperparameters	BulletGym	SafetGym	MetaDrive
Common			
Training Steps	100k	100k	200k
Policy network architecture	[512, 512] MLP	[512, 512] MLP	[512, 512] MLP
Cost thresholds for main results	(10, 20, 40)	(20, 40, 80)	(10, 20, 40)
Seeds for main results	(0, 10, 20)	(0, 10, 20)	(0, 10, 20)
BCR			
Algorithm Version	Stochastic	Stochastic	Deterministic
Batch Size	512	512	512
Optimizer	Adam	Adam	Adam
Learning Rates $\lambda_Q^C, \lambda_V^C, \lambda_Q^R, \lambda_V^R, \lambda_{\pi_C}, \lambda_{\pi_R}$	0.0003	0.0003	0.0003
Target Update α	0.005	0.005	0.005
Discount factors for cost and reward γ_C, γ	0.99	0.99	0.99
Expectile for cost (IQL) τ_C	0.2	0.3	0.5
Expectile for reward (IQL) τ_R	0.5	0.6	0.5
Budget sample count n	1	1	1
Policy dropout	0.1	0.1	0.1
AWR Temperature for both cost and reward (IQL) β	3	3	3

Table 10: Default Hyperparameters of BCRL for tasks in three environments.